The Institute of Space and Astronautical Science
Report No.666, February 1997

Meteoroid and Space Debris Impact Investigations in SFU Post Flight Analysis Activities: Preliminary Results and Further Directions

By

Kyoichi KURIKI*, Mitsuru TAKEI**
Noboru WAKASUGI*** and Tetsuo YASAKA****

(October 24, 1996)

ABSTRACT: This report explains early post flight analysis (PFA) operations of the Space Flyer Unit (SFU) spacecraft within the first 6 months after its retrieval from the Low Earth Orbit in January 1996. The special emphasis is given to hypervelocity impact signatures by meteoroids and space debris and surface contamination assessment. Brief reviews are also given for scientific rationales of the PFA activities, meteoroid and debris characteristics, hypervelocity impacts on various spacecraft materials, previous dust detectors and PFAs and the description of the mission profile and components of the SFU. Its on-going impact investigation is in good progress and producing abundant impact data mainly on Kapton MLI and Teflon targets. In total 337 impacts were recorded through various visual inspections, with the detection limit of several hundred μm, depending upon the target materials. Preliminary flux and size distributions of impacts are studied. Detailed CCD scanning will be the next step with as small detection limit of crater/hole sizes as ~200 μm. Calibration impact experiments for the surface materials are also in progress. By completing the impact data base, this will be Japan's first contribution for the near Earth dust environment studies and is hoped to be open to the international research community.

1. INTRODUCTION

The Space Flyer Unit (SFU) is Japan's first unmanned, reusable, free-flying space platform which was developed by the inter-ministerial joint effort, namely amongst the Institute of Space and Astronautical Science (ISAS) of the Ministry of Education, Science, Sports and Culture (MOE), the New Energy and Industrial Technology Development Organisation (NEDO) / the Institute for Unmanned Space Exper-

* Institute of Space and Astronautical Science, 3-1-1 Yoshinodai, Sagamihara, Kanagawa, 229 Japan
** National Space Development Agency of Japan, 2-1-1 Sengen, Tsukuba, Ibaraki, 305 Japan
*** Institute for Unmanned Space Experiment Free Flyer, 2-12 Kanda-Ogawamachi, Chiyoda-ku, Tokyo, 101 Japan
**** Department of Aeronautics and Astronautics, Kyushu University, 6-1-1Hakozaki, Higashi-ku, Fukuoka, 812 Japan
Representative of the Meteoroid and Debris Impact Investigation Group (M&D IIG) under the Japan Society of Aeronautical and Space Science (JSASS)

iment Free Flyer (USEF) of the Ministry of International Trading and Industry (MITI), and the National Space Development Agency (NASDA) of the Science and Technology Agency (STA). The spacecraft was 4.46 m octagonal in diameter by 3.0 m height. The SFU "mission-1" system was launched by the third H-II rocket on 18 March 1995. Its mission objectives included the successful retrieval of the spacecraft, verification of its flight system, environmental validation for the follow-on SFU missions and the implementation of scientific, engineering and observation experiments. Since the spacecraft was exposed in space environment about 10 months (~301 days or ~2.6 x 10^7 seconds), post flight inspection of the surfaces was of great interest for meteoroid and space debris impact studies.

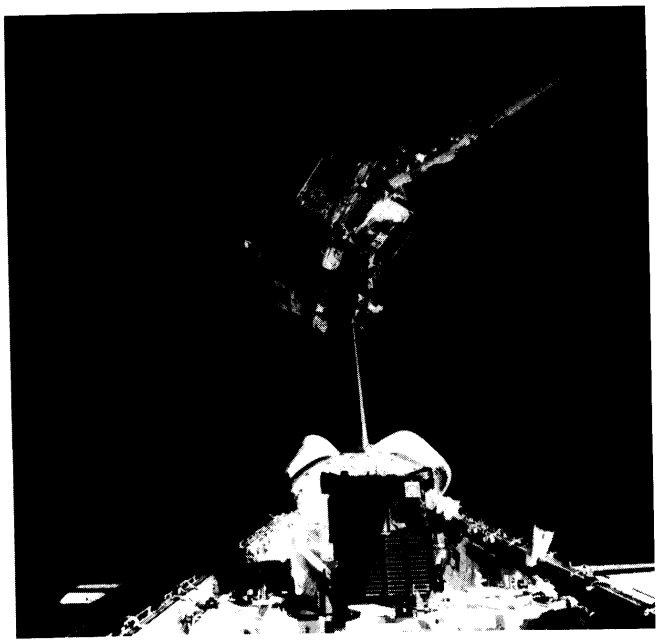

Fig. 1 SFU spacecraft retrieved by the shuttle orbiter Endeavour in the mission STS-72 (Photo courtesy: NASA)

After all the objectives were accomplished, except having both Solar Array Paddles (SAP) jettisoned by failing the confirmation of latching signals before retrieval, the SFU spacecraft main body was captured by the space shuttle Endeavour (STS-72 mission) on 13 January 1996 (Fig. 1). After landing at the NASA Kennedy Space Centre (NASA/KSC) in Cape Canaveral, Florida on 20 January, visual inspections of the whole spacecraft, which were proposed and planned by the Meteoroid and Debris Impact Investigation Group (M&D IIG) under the Japan Society of Aeronautical and Space Sciences (JSASS), were conducted for three times jointly by the SFU project members and the M&D IIG. The first inspection was performed at NASA/KSC in January, the second at the Astrotech Space Operations Company (ASO) at Titusville, Florida in February, and the third at the Mitsubishi Electric Corporation (MELCO) in Kamakura, Kanagawa, Japan in April. After deintegration of the spacecraft in May, more detailed inspections and other preparatory activities for subsequent digital scanning were conducted at manufacturer and ISAS facilities where each component was stored. Throughout these activities, the number of the impacts on selected surfaces of various components were visually counted and the sizes of the major damages were measured. This report describes preliminary results obtained during these initial investigations and summarises analysis plans for further studies.

2. METEOROIDS AND SPACE DEBRIS

2-1. METEOROIDS

Cosmic dust that are gravitationally bound to the Solar System are referred to as "meteoroids" or "interplanetary dust particles (IDP)". They originate mainly from asteroids and comets, with minor contributions from β-meteoroids and impact ejecta from planets and satellites. The existence of meteoroid clouds has been long known from the zodiacal light and meteor showers. More recently IRAS and COBE satellites discovered a heliocentric dust ring along the Earth's orbit that are considered to be asteroidal origin (Dermott *et al.*, 1984 and 1993 and Reach *et al.*, 1995). Also recent interplanetary missions i.e., Ulysses and Galileo (e.g. Grün *et al.*, 1993) and ground radar meteor observation by AMOR (Taylor *et al.*, 1996) have indicated the presence of the interstellar particles (ISP) inside the Solar System. Even after a century since the first collection of micrometeorites by the British Discovery Expedition, those sampled from the terrestrial environments, i.e. stratosphere, deep sea sediments and polar blue ices, still suffer from physical and chemical alterations and selection biases. Unlike the constantly changing the Earth's surface, by meteorological and by geological interactions, meteoroids in space are free from such effects and biases and can preserve much information of their origins. They are thus relics from the early history of the Solar System, from the inner planet regions to the Oort-Öpik Cloud.

2-2. SPACE DEBRIS

There is yet another dust population in the Low Earth Orbit (LEO): "space debris", namely non-operational artificial objects produced through various activities in space (e.g. Johnson and McKnight, 1987 and National Research Council USA, 1995). Since the USSR's Sputnik-1 in 1957, ground observations have tracked over 24,000 artificial objects. As of early 1995, there are nearly 8,000 artificial objects in orbits but only 6 % of those are operational satellites (Jehn, 1995). Tracking capability of ground-based optical and radar observations for moving objects around the Earth are limited by size in the order of cm. In the diameter range of 1-10 cm, the estimated dust population in the near Earth environment increases to 4×10^4 - 1.5×10^5 and even smaller debris dominate the total dust population except the range of 10–100 μm (Kessler, 1991). By assuming the annual debris mass growth rate of 5%, it makes the debris population in LEO exceed meteoroids at all size ranges by the year 2010. The increasing quantity of debris clouds leads to "cascading" collisions on orbiting objects including operational satellites. Secondary break-ups could produce a greater quantity of debris accumulating in the most heavily used orbits and the result could be that further satellite utilisation would be effectively impossible for the foreseeable near future.

2-3. POST FLIGHT ANALYSIS

Therefore, apart from biased collection of micrometeorites in the terrestrial environment, studies of micrometeoroids and space debris of <1 cm in size in the near Earth space is only possible by in-situ detection and collection on spacecraft. Through this research, meteoroid studies will contribute to the understanding of the origin and evolution of the Solar System while identifying orbital debris impacts will help to assess the potential danger of fatal impacts on operational satellites and improve future spacecraft designs as an interest in the space development.

The number of dust impacts is essentially a function of exposed time and exposed surface area of the spacecraft. Large, flat components made from uniform materials on such spacecraft include multi-layer insulation (MLI) thermal blankets, solar cell arrays (SCA) and aluminium (Al) frames and they serve as "passive dust collectors". At NASA, post flight analyses (PFA) of returned samples started since the Gemini-Apollo-Skylab era and currently shuttle orbiter windows are also scanned in a regular inspection.

In the last decade, post flight analyses (PFA) of large and long exposed spacecraft, such as NASA's Long Duration Exposure Facility (LDEF) (See *et al.*, 1990), ESA's European Retrievable Carrier (EuReCa) (UniSpace Kent, 1994) and the Hubble Space Telescope (HST) solar cell array (SCA) (Space

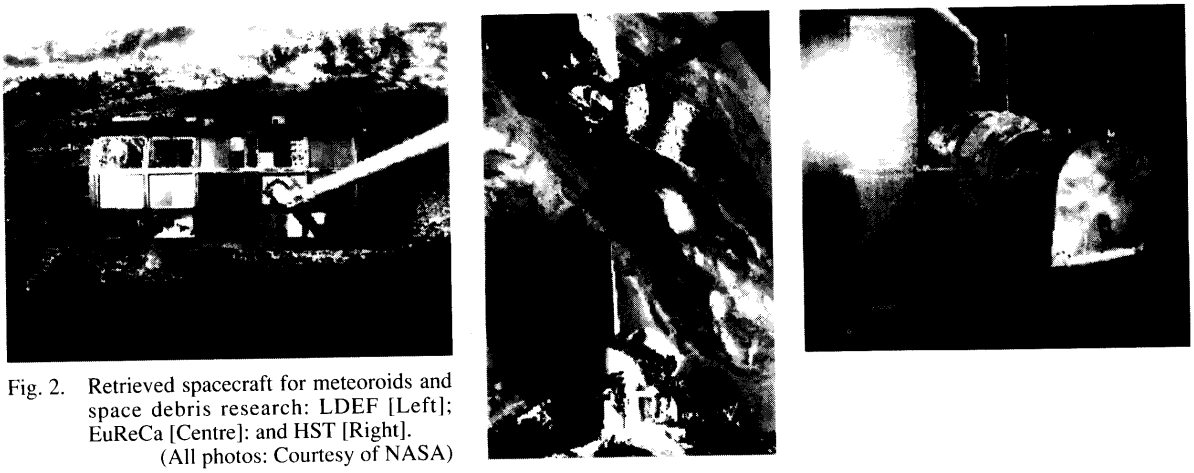

Fig. 2. Retrieved spacecraft for meteoroids and space debris research: LDEF [Left]; EuReCa [Centre]: and HST [Right]. (All photos: Courtesy of NASA)

Applications Services, 1995), have been extensively carried out after they were returned to the ground by space shuttles (Fig. 2). Apart from meteoroid and debris impacts, the previous PFA activities have also enhanced our knowledge of material alteration such as erosion, outgassing, discoloration, oxidisation and welding by the space environment effects including high vacuum, solar radiation (i.e. ultraviolet (UV)), high energy particle bombardment, extreme thermal cycle and atomic oxygen (AO).

3. HYPERVELOCITY IMPACTS

3-1 Definitions

The majority of surfaces of retrieved spacecraft experienced "hypervelocity impacts (HVI)" by meteoroids and space debris. Two common criteria of HVI phenomena are: (1) an impact whose projectile velocity exceeds the speed of sound of a target material at its initial contact so that shock waves are generated; and (2) an impact whose velocity is fast enough to release so large energy impulse that a target material phase changes from solid to fluid states (or even vaporisation and ionisation). The "HVI morphology" is thus referred to when target materials indicate evidences of phase change and/or (low velocity) reaction to shock propagation induced by HVI impulse such as cracks, rear face spallation and shape deformation like crater lips.

The HVI morphologies are normally classified into the following categories:

(1) Crater: A substantial excavation of the target material without punctuation

(2) Marginal Perforation: A target just perforates and rear face spallation occurs

(3) Complete Penetration: A projectile completely passes through the finite thick target.

Thus there is a gap between parameters we can measure from those impact features and what we

[What We Can Observe] Impact Features on Space Exposed Surfaces	[What We Wish to Learn] Origins of Impactors: Natural or Artificial
• Crater / Perforation Characteristics - Diameter - Depth - Circularity / Irregularity - Impactor Remnants - Phase Change • Direct / Secondary Impacts - Spatial Distribution - Impact Direction	• Projectile Materials - Size - Density - Shape - Composition • Impact Velocity • Impact Angle / Direction

Table 1. Comparison between available data and research goals

Particles	Natural---------"Meteoroids"	Artificial-------"Space Debris"
Origins	• Asteroids / Comets • ß-meteoroids • Ejecta from planets and satellites • Inter-Stellar Particles (ISP)	• Non-operational space instruments • Break-ups, Collisions, Fragmentation • By-products of spacecraft operations • Surface degradation
Dynamics	Unbound to Earth (Omni-Direction)	Bound to Parent Body Orbits
Velocity w.r.t. Earth	• Streams: Up to 70 km/s • Sporadic: Average 20 km/s • ISP: Can be > 100 km/s	• Circular in LEO: ~8 km/s • GTO: Varies with perigee altitude • Circular in GEO: ~3 km/s

Table 2. Comparison between meteoroids and space debris

eventually wish to learn: the origins of impactors (Table 1). As can be seen in Table 2, there are clear criteria to distinguish meteoroids from orbital debris if we can measure velocity, direction, time of arrival and composition of impactors. Yet all the flight data employed in PFAs usually come from "passive collectors", as opposed to "active detectors". Thus in order to correctly separate meteoroids and debris, one must develop empirical scaling laws, by understanding how HVIs could change physical and chemical properties of the impactors.

3-2. Measuring Parameters

As can be seen in Figures 3 to 8, the following parameters are widely accepted for conventional ductile and brittle materials (e.g. Yano, 1995).

For ductile targets (e.g. metals) in Figures 3–5:

(1) Crater Diameter (Dc): The diameter of the inner edge of the impact crater at the sample surface.

(2) Crater Depth (P): The depth from the target surface to the deepest bottom of the crater.

(3) Hole Diameter (Dh): The diameter of the impact perforation.

(4) Target Thickness (T)

By the T/P ratio, targets can be classified as (1) "semi-infinite thickness" (T >> P), (2) "finite thickness" (T ≥ P) and (3) "thin" (T < P). As T/P decreases, finite thickness targets have rear face spallation by release of shock wave. At T/P ≈ 1, the bottom of the crater forms a marginal perforation. In the case of T/P << 1, Dh becomes comparable to Dc as a complete penetration. At a fixed impact velocity of 6 km/s, Dh becomes nearly equal to the diameter (d) of an impactor and represents its outline like a "cookie puncher" at Dh/T > 50 (Hörz *et al.*, 1994a).

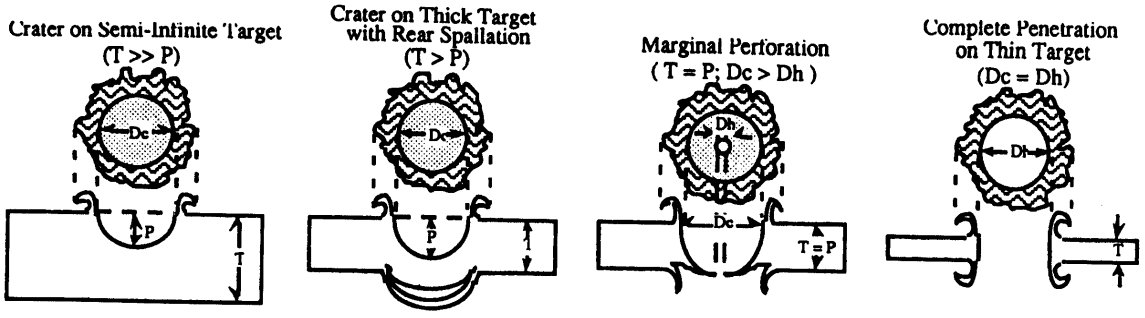

Fig. 3 HVI features on metals in different thickness of targets to a crater size

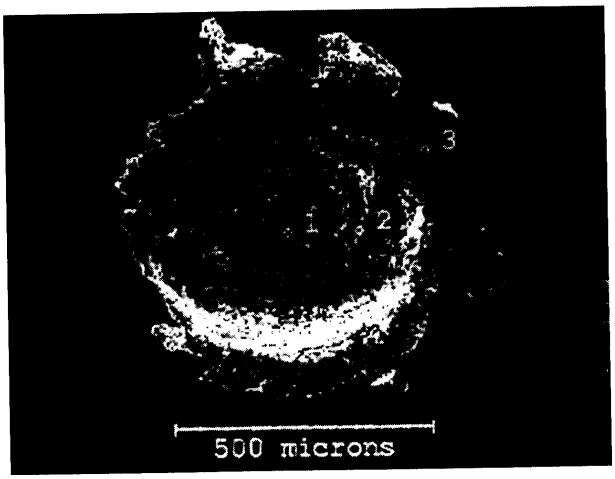

Fig. 4 SEM image of a crater on LDEF thick Al clamp: Dc = 458 x 444 μm (Photo courtesy: H. Yano)

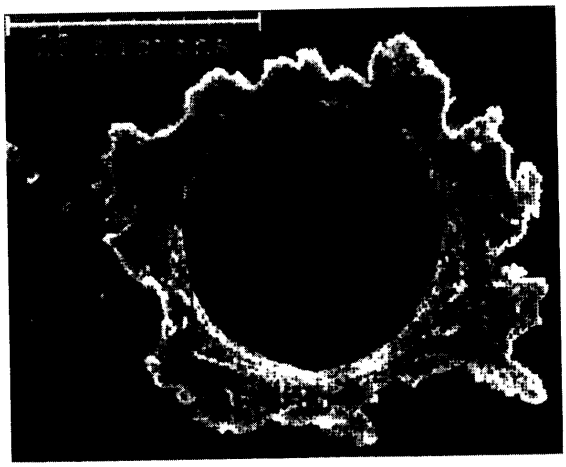

Fig. 5 SEM image of a circular, complete penetration hole on a 9 mm-thick Al foil of TiCCE experiment on EuReCa: Dh = 25.2 μm (Photo courtesy: H. Yano)

For brittle materials (e.g. glass and solar cells) in Figures 6–8:

(1) Central Pit Diameter (Dp): This is the core information of an impactor size.

(2) Shatter Zone Diameter (Ds): This is a highly fragmented shocked zone surrounding Dp where final 'powdering' leads to an efficient light scattering.

(3) Conchoidal Spallation Diameter (Dco): Under tensile stress brought by the uplifting of the central pit and by propagation of shock wave, a brittle target demonstrates a conchoidal fracture with the spallation of platelets. The platelets are "mussel shell"-like circular features. It is much larger than Dp and Ds and thus used as a reference parameter for the size distribution. It also may indicate crater ellipticity and impact directionality for some cases.

(4) Maximum Damage Diameter (Dm): This shows the final stress release and the degree of mechanical damage of the target to the maximum extension, excluding radial cracks.

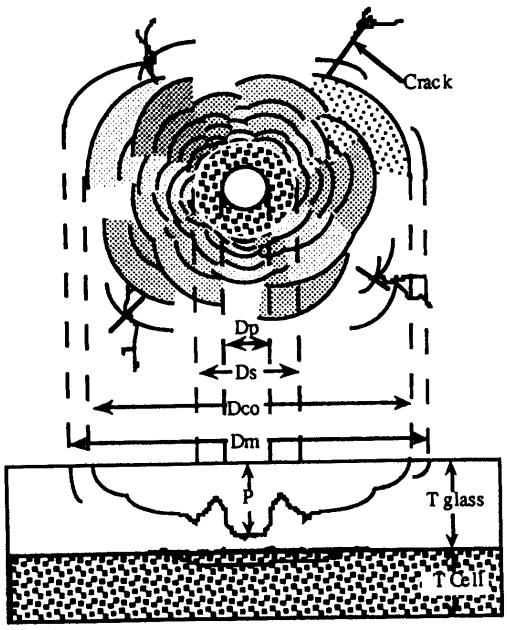

Fig. 6 HVI features on solar cells

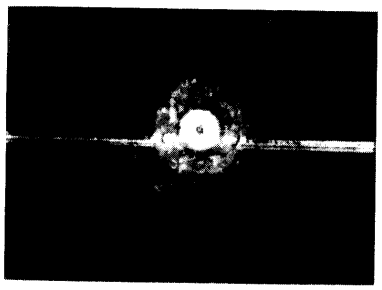

Fig. 7 A circular crater on the EuReCa solar cell (F5f73) of Dp = 60 μm and Dco = 760 μm at magnification (mag.) x100. (Photo Courtesy: ESA)

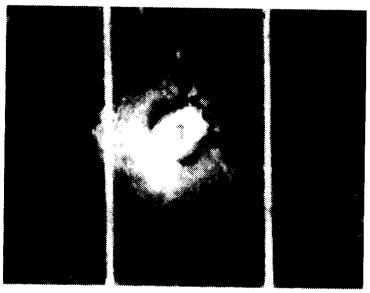

Fig. 8 An elliptical crater on the HST solar cell (FEE-7pD33-GT) of Dp = 240 μm, Dco = 910 μm and circularity index (Ci) = 0.66 at mag. x100. It was caused by a inclined impact at a modest incident angle (≥40° from the normal). In both the images, an interval of two silver electrodes is 1.25 mm. (Photos courtesy: ESA)

As for MLI (e.g. 10 μm-order thick aluminised (Al) Kapton films), there are only complete penetration holes (Dh) being measurable from the surface (Fig. 9). Other large, flat components of general spacecraft include laminar structure of metalled Teflon radiators (Fig. 10) and thermal control painted (e.g. Ti) aluminium plates such as scuff plates for shuttle interface (Fig. 11). Painted metal plates of LDEF and EuReCa had central craters on exposed metal surfaces surrounded by circular spalled zone of the top paint. Silverised (Ag) Teflon radiators of the Ultra-Heavy Cosmic Ray Experiment (UHCRE) on the LDEF indicated ring-featured impact damages where a central crater fractured the surface lamina and atomic oxygen intruded and oxidised metal coating underneath due to shock wave propagation (Mullen and McDonnell, 1994). Through the SFU PFA, we have determined measuring parameters of these components as follows: Dh = hole diameter (inside the hole lip) for the MLI; Dp = central pit crater diameter, Dc = main crater diameter (hollow part), Dr = rim diameter (lamina entry), and Dm = maximum damage diameter (outer-most ring) for the Teflon; and Dc = central crater diameter and Dsp = spalled paint diameter for the painted Al plates (also see Yano *et al.*, 1996). SFU has all of these surfaces and it is important to cross-calibrate the "targets" with metal and glass impacts so that comparison of flux and estimated impactor size becomes possible with the previous PFA results.

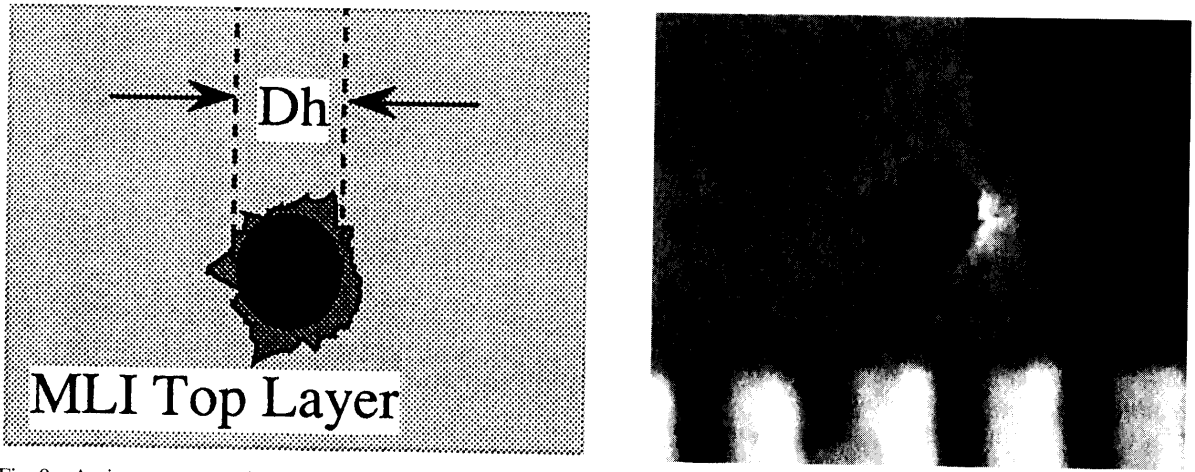

Fig. 9 An impact penetration on Al Kapton MLI: (Left) Parameter definition; (Right) An impact on the SFU SEM rear face MLI of Dh = ~300 μm (scale unit = 500 μm) (Photo courtesy: Denso)

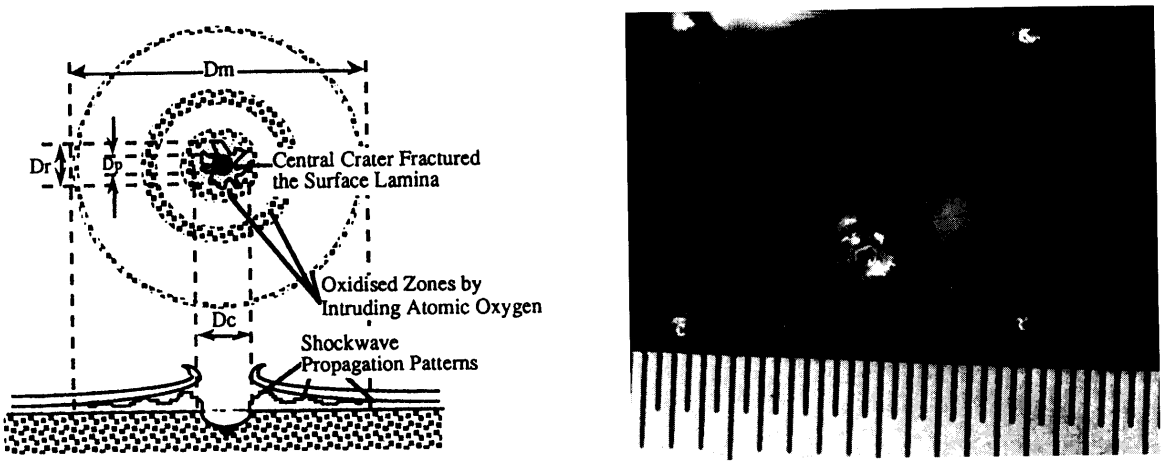

Fig. 10 An impact crater on Ag Teflon radiator: (Left) Parameter definition; (Right) An impact on the SFU PLU-4 Teflon radiator of Dm = ~5 mm (scale unit = 500 μm) (Photo courtesy: ISAS)

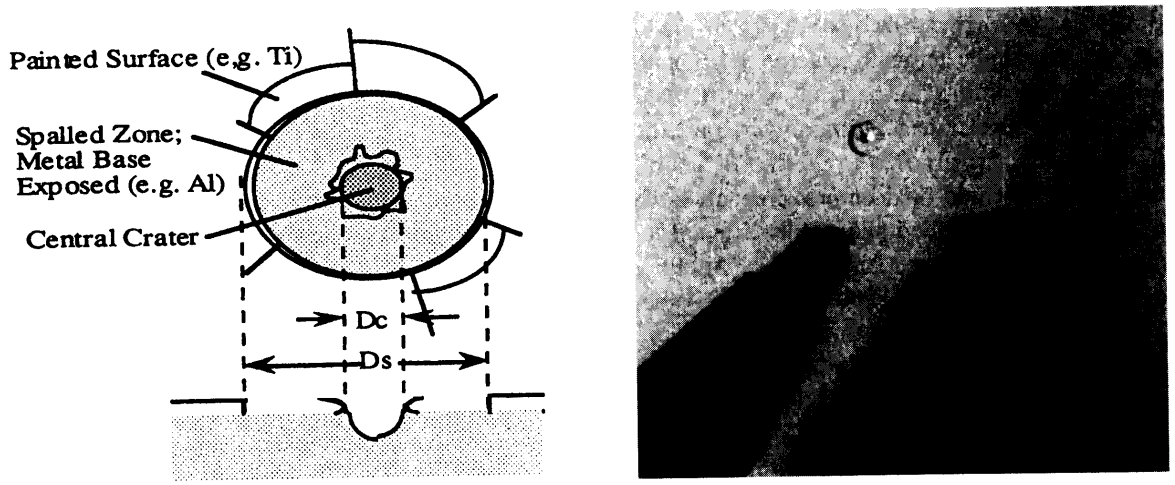

Fig. 11 An impact crater with spalled thermal protection paint on an Al plate: (Left) Parameter definition; (Right) An impact on the SFU Al scuff plate (-Y/Low) of Dc = ~200 μm and Dsp = ~600 μm (Photo Courtesy: ISAS)

4. PREVIOUSLY RETRIEVED SPACECRAFT

4-1. Flux Evaluation

The impact flux must be properly interpreted with the spacecraft's attitude, orbital parameters, mission epoch and geometrical effects as well as local contamination by the spacecraft itself and its deployed and retrieved vehicles. To distinguish between meteoroid and space debris impacts, this PFA work includes both a physical qualitative approach and a chemical qualitative approach to the data. For the physical approach, an impact fluence to each examined surface is converted into a cumulative impact flux per unit area (m^2) per unit time(s), then estimated a common parameter of impact effectiveness, for example, Fmax, an equivalent thickness of an aluminium plate to produce a marginal perforation (e.g. Carey, McDonnell and Dixon, 1985). For each target sample, morphological information is carefully studied for the connections with size, directionality and other physical parameters of the impactors. For chemical (or "elemental") analysis, impact residue surveys with an energy dispersive X-ray spectrum analyser (EDX)

are the common first step for determination of their origins.

In case of man-made space debris, primary interest is the rate of impact onto a unit area of space assets, or debris flux, as a function of location (altitude and longitude), direction and impactor size. In most of cases where attitude of retrieved spacecraft is identifiable, the raw plot of the cumulative flux is the desired output. If the attitude of the spacecraft is not constant while in orbit, as is the case with SFU, the measured data should be corrected accordingly.

In case of meteoroids, the situation is somewhat different and more complex. Once we obtain a raw plot of the cumulative flux Φ against Fmax or impactor size (d), the flux must be corrected by various factors (Table 3). Where $f_{\oplus}$ is the meteoroid flux near the Earth and $f_{ip}(1)$ is the meteoroid flux at 1 AU without the Earth, Φ(Fmax) is given as

$$\Phi(\text{Fmax}) = Q_{ss}\, Q_{fd}\, Q_{vs}\, Q_{mc}\, f_{\oplus} = [Q_{ad}\, Q_{ge}\, Q_{es}\, Q_{ss}\, Q_{fd}\, Q_{vs}\, Q_{mc}]\, f_{ip}(1) \quad (1)$$

Fig. 12 illustrates major factors that alter impact fluxes on space exposed surfaces. Among those

Location of Effects	Flux Changing Factor	Notion
In LEO	Atmospheric Drag	Qad
	Gravitational Enhancement	Qge
	Earth Shielding	Qes
On Spacecraft	Spacecraft Shielding	Qss
	Face Dependence Enhancement	Qfd
On Impact Targets	Velocity Sensitivity Enhancement	Qvs
	Material Conversion to Al 1100-0	Qmc

Table 3 Summary of factors that change the interplanetary space flux model at 1 AU (i.e. Divine *et al.*, 1993) with actual observed /collected influx of meteoroids to the near Earth space.

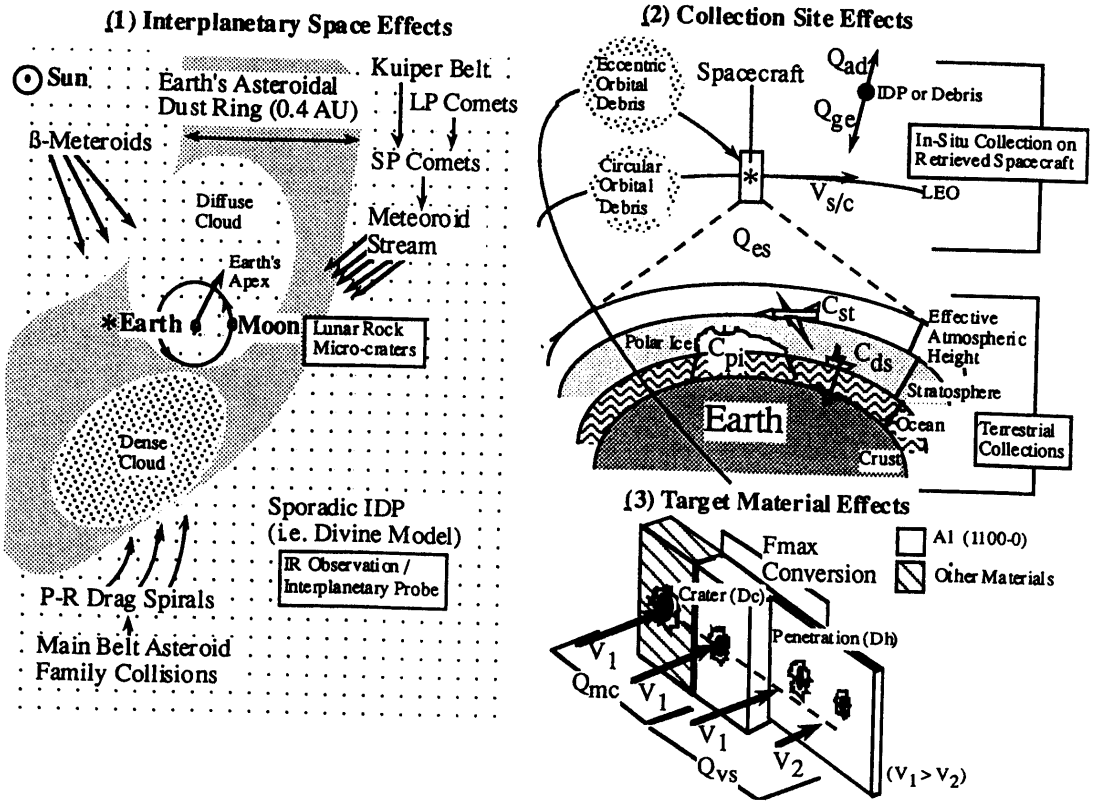

Fig. 12 Summary of flux alteration factors for meteoroids and space debris (from Yano, 1995)

factors, the collection factors of each territorial collection site (stratosphere (C_{st}), polar ice (C_{pi}) and deep sea sediments (C_{ds})) are not investigated here because it is beyond the scope of this study. They are all functions of the geocentric particle velocity (V_{pg}), particle density (ρ_p), tensile strength (σ_p) and d on the top of other factors based on survivability, collection efficiency and selection effect of particles at each site.

4-2. Brief History of Post Flight Analyses

The first attempt of dust detection at high altitudes was made by sounding rockets but the exposure time and area product was too small to have a sufficient flux of measurable size particles (McDonnell, 1978). Later various detection techniques were developed and impact ionisation detectors and penetration sensors were particularly sensitive (mass limit $\approx 10^{-17}$ g) (Zook, 1992). The Helios-1 spacecraft carried impact plasma detectors in interplanetary space in 1976; this expertise has now been succeeded by a fleet of "new generation" interplanetary probe such as Giotto, Galileo, Ulysses, Hiten, Planet-B and Cassini.

As opposed to such "active detectors", a simpler but still reliable technique to study impact flux is "passive collectors" and PFA of returned components. These do not have a capability to measure the dust flux as a function of time and altitude but only integrate all the impacts over the whole exposed time in the range of altitudes they orbited. Since 1981, space shuttles have revolutionised the accessibility to space exposed samples by salvaging whole or parts of satellites. Also short duration dust impact experiments have become possible on the cargo-bay pallet or the Canadarm. Table 4 and Fig. 13 summarise mission

Spacecraft	SMM	LDEF	EuReCa	HST SCA
Exposure Duration	131 x 10^6 s 4.15 years	182 x 10^6 s 5.78 years	28.2 x 10^6 s 0.89 years	114 x 10^6 s 3.62 years
Median Epoch	14/03/1982	24/02/1987	12/01/1993	02/03/1992
Epoch Difference*	-4.95 years	0 years	+5.88 years	+5.01 years
Scanned Area	2.84 m^2	80.7 m^2	105.4 m^2	47.1 m^2
Altitudes: Initial Final Mean / Operational	570 km 500 km 560 km	477 km 326 x 335 km 458 km	426 km 476 km 502 km	614 km 594 km 610 km
Pointing Attitude	Sun	Earth	Sun	Sun/Observing Objects

Table 4 Summary of retrieved spacecraft data (* = with respect to LDEF's mean epoch). SMM = Solar Maximum Mission satellite.

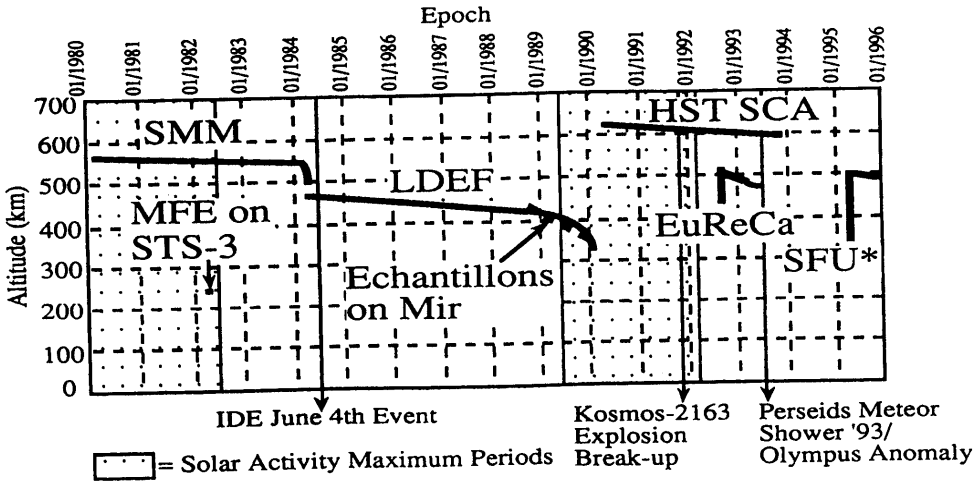

Fig. 13 Summary of altitude and epoch profiles of the retrieved spacecraft (from Yano, 1995)

profiles of spacecraft carried such passive collectors and/or conducted their PFA activities in the last decade. Detailed review of major results of the past PFAs is available elsewhere (i.e. Yano, 1995). Note that the median epoch of HST is earlier than that of EuReCa. Among these spacecraft, LDEF is the only gravity gradient stabilised satellite at the solar activity maximum period.

5. SFU MISSION PROFILE SUMMARY

The SFU spacecraft was launched on 18 March 1995 via the H-II launch vehicle from the NASDA Tanegashima Space Centre Launch Site into a 330 km circular orbit. After the solar array paddles (SAPs) were deployed and a part of the core system was checked out, the spacecraft performed orbit change manoeuvres five times to raise itself to its operational altitude of 482 km. After it reached the mission orbit on 23 March, a thorough checkout took place and experiments were activated. SFU began its science mission operations on 29 March. In the first operational month, the "Infrared Telescope in Space" (IRTS) observation and space biology experiment (BIO) were conducted through 26 April. During this period, the attitude was controlled for observing targets of the IRTS. After completion of the observations, the science and technology experiments, engineering tests for Japan Experiment Module-Exposed Facility (JEM-EF) in the International Space Station Alpha (ISS) and three furnaces experiments for microgravity material sciences were performed for nearly four months. The spacecraft altitude was maintained in 482 km most of the time, in which the attitude was controlled by the reaction wheels to make the SAPs face to the Sun. Thus the SAPs always pointed to the Sun while the -Y wing always pointed to the celestial northern hemisphere such that the +Z face preferentially headed to the apex of the Earth's heliocentric motion (Fig. 14).

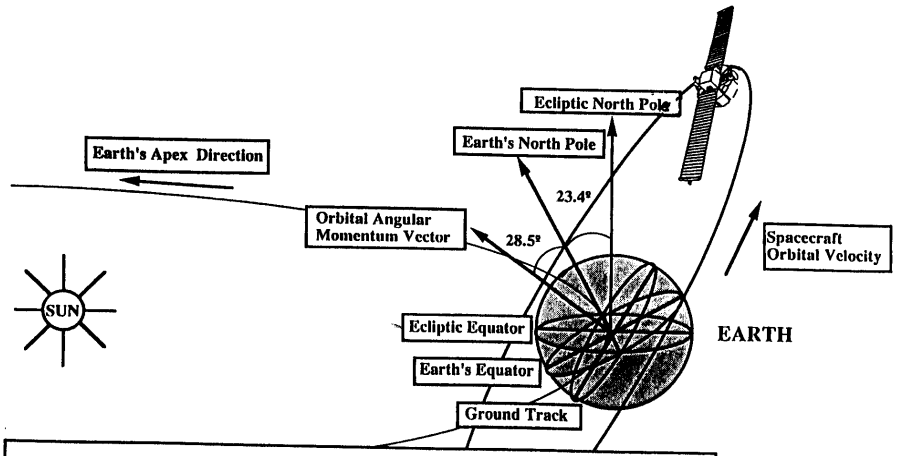

Fig. 14 Orbital geometry of SFU spacecraft

The science mission phase completed on 31 August. Then the mission proceeded to experimental operations for the core instruments and preparation for its shuttle retrieval. During this phase, the SFU attitude was controlled mostly in the nominal or Sun-pointing modes using the reaction control system, except for during the orbit maintenance manoeuvres. On 13 January 1996, the spacecraft was retrieved at an altitude of ~480 km by the Remote Manipulator System (RMS, or "Canadarm") of the shuttle orbiter Endeavour which was operated by the STS-72 mission specialist Koichi Wakata. Prior to the capture, the

both SAPs were jettisoned due to a signal failure to reconfirm the latching signals after their retraction. The overall operation sequence of the SFU is illustrated in Fig. 15.

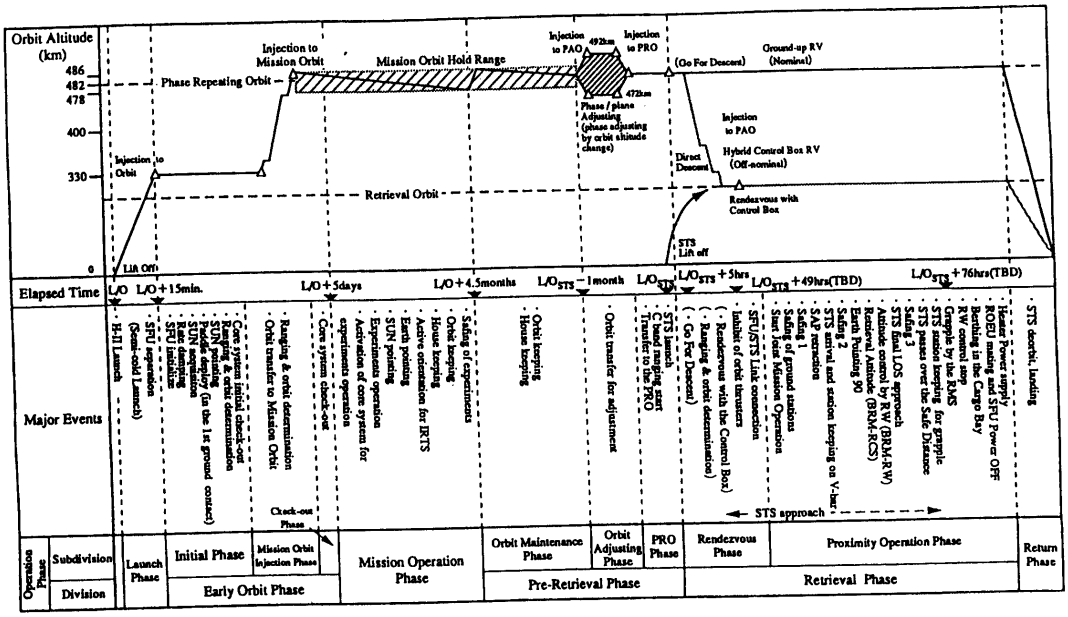

Fig. 15 SFU operation sequence and major events in orbit

6. SFU SPACECRAFT COMPONENTS

The SFU spacecraft "mission-1" configuration was octagonal in shape with two SAPs. Five modular payload units (PLU-1, 2 and 4 and BSU-1 and 2) and two special payload units (SPLU-1 and 2) were accommodated on the spacecraft. The launch mass of SFU was 3850 kg, 900 kg of which were payloads. The main body structured 4.46 m in diameter and the normal length of 3.0 m. Each SAP was 24.4 m tip-to-tip in size when fully deployed. The total exposed area was ~146 m^2. The external view of the SFU and its functional block diagram are shown in Figures 16 and 17, respectively. Except for a very few surfaces, the spacecraft was covered with MLI thermal blankets (Al Kapton polyimide outer layer) and perforated, silverised (Ag) Teflon thermal control radiators.

Electrical power for the SFU sub-systems during the mission was provided by the two SAPs and four rechargeable batteries. SFU had an S-band command and telemetry system used to communicate

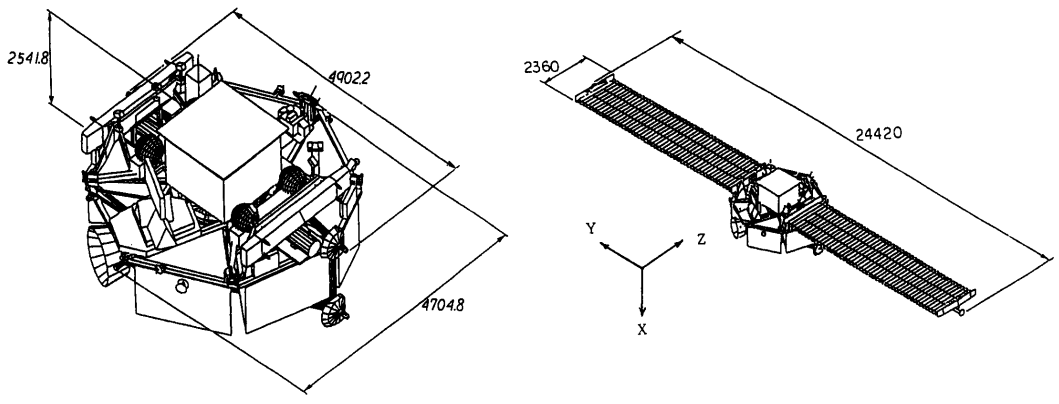

Fig. 16 SFU spacecraft configuration and dimension (unit: mm)

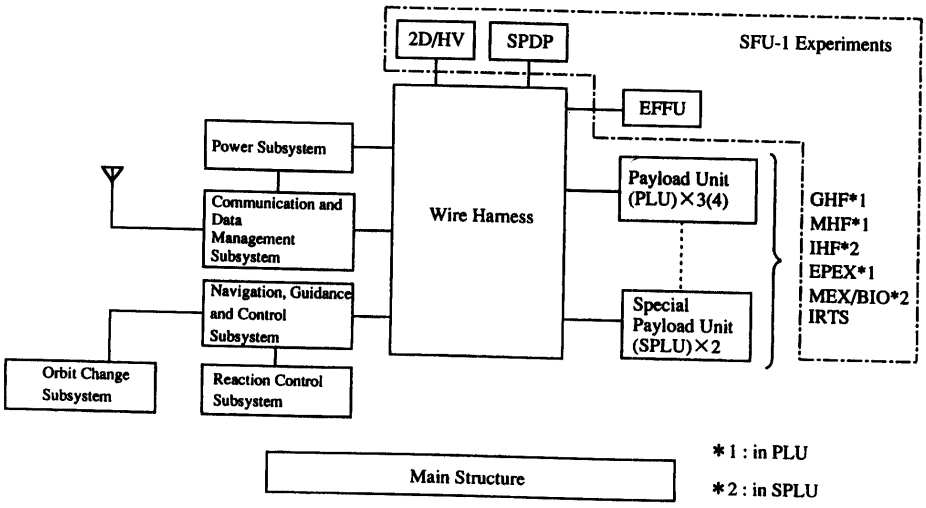

Fig. 17 SFU functional block diagram

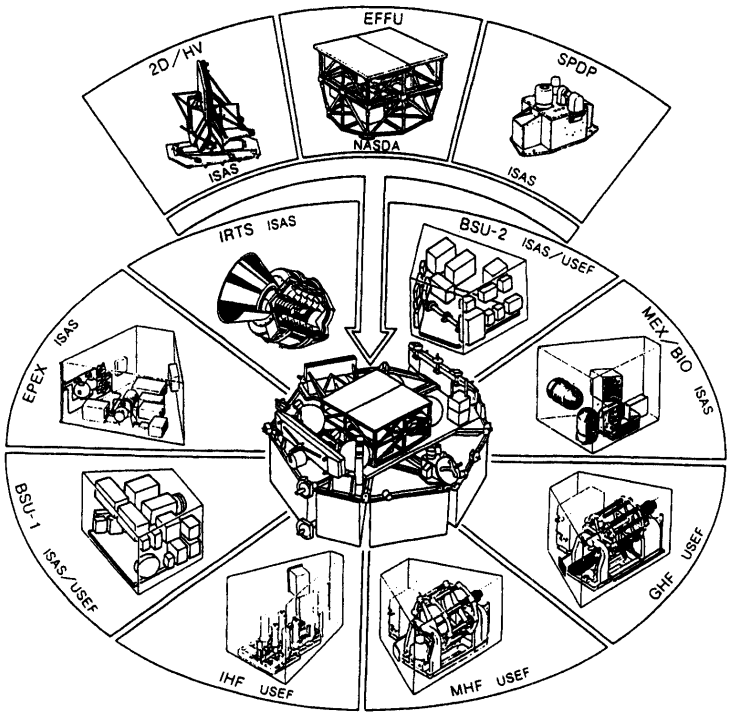

Fig. 18 SFU experiments and their locations

with ground stations and the shuttle orbiter. Attitude control in the normal mode was via Sun-pointing by reaction wheels unloaded by thrusters. The Reaction Control System (RCS) consisted of twelve 3N-thrusters and four 23N-thrusters and used mono-propellant hydrazine. Orbit control manoeuvres were accomplished using the onboard guidance and navigation systems of the navigation, guidance and control computers, the global positioning system, the inertial reference unit and accelerometer. Eight 23N-thrusters were used to manoeuvre the spacecraft.

Passive thermal control was provided by the MLIs and Teflon radiators while active control was achieved by thermal louvers, heat pipes and controlled heaters. The Space Environment Monitoring sys-

tem (SEM) on the Sun face consisted of vacuum gauges, a mass analyser, plasma probes, potential detectors, wave receivers and microgravity meters. It also carried eight pieces of test materials exposed to the space environment.

The experiment instruments were accommodated in the payload units (PLU) or installed on the exposed upper deck, called the Exposed Facility Flyer Unit (EFFU). There were 10 experiments in total; Two-Dimensional High Voltage Solar Array (2D/HV: by ISAS), IRTS (by ISAS), Electric Propulsion Experiment (EPEX: by ISAS), Material and Space Biology Experiments under Microgravity (MEX/BIO: by ISAS), Space Plasma Diagnostic Package (SPDP: by ISAS), EFFU (by NASDA), Gradient Heating Furnace (GHF: by USEF), Mirror Heating Furnace (MHF: by USEF) and Isothermal Heating Furnace (IHF: by USEF) (Fig. 18).

7. PRE-LANDING ESTIMATE OF DUST IMPACT FLUENCE

7-1. Calculated Impacts on SFU

Prior to its launch, expected impact fluence on the SFU in the nominally planned period of 6 months was simulated with the computer software called "ESABASE/DEBRIS" by Yano and Kibe (1994). The ESABASE/DEBRIS is a 3-D numerical analysis software for micrometeoroid and space debris impact risk assessment on an arbitrary spacecraft in LEO developed by ESA. It takes account of geometrical and directional effects such as shielding and trajectory direction of impactors. Models of population and orbital dynamics of micrometeoroid were developed by NASA in 1990 based on E. Grün and N. Divine's works. It assumes omni-directionality and isotropic distribution of the micrometeoroid near the Earth and seasonal meteor showers give an increase of the flux. The solar activity cycle was also considered. The space debris model was based on D. Kessler's work but the discovery of debris impacts counted 15 % of the entire impacts on the trailing edge of the LDEF was not implemented yet. The debris mass growth rate was assumed 5 % per year while its fragmentation growth was 2 % annually.

The nominal altitude of SFU was set 482 km with 28.5° orbital inclination. The operation was assumed to start on 1 February 1995. The minimum size of space debris to be detected was 10 μm diameter whilst the mass detection limit of micrometeoroid was 10^{-9} g. Estimated areas of the SAPs, EFFU side and peripheral faces of the payload units were 46.56 m^2, 5.98 m^2 and 13.62 m^2, respectively. Table 5 shows the number of impact events expected on each component in the 6-month mission duration. Note that all impacts are not necessarily to form HVI craters or perforations. As can be seen, SAPs would have provided impact data of around 8000 meteoroids and about the same number of man-made debris in those size/mass limit, if they were recovered.

Major Surfaces	Meteoroids (>10^{-9} g)	Space Debris (> 10 μm)
SAPs (Sun Face)	4321~3920	4249~3824
SAPs (Anti-Sun Face)	3862~3551	4036~3611
EFFU Sides	374~334	436~382
Payload Unit Peripheral Faces	1106~1015	1324~1200

Table 5 Expected number of impacts on SFU components in 6 months from 01/02/1995 (the nominal plan)

7-2. Pre-launch and In-orbit Monitoring

Pre-launch inspection of the spacecraft was limited to manufacturing defects and contamination assessment. Brief in-orbit monitoring was made for power production rate of SAPs but no significant degradation due to impacts was recognised. During the retrieval mission, snap shots were taken by astronauts for visual inspection of large morphological alteration. Apart from severe discoloration on the Sun-pointing faces, the spacecraft showed no such signs.

8. INITIAL POST FLIGHT INSPECTIONS AT NASA/KSC

8-1. PFA Operation Sequences

General procedures of spacecraft PFA have been developed through experiences on LDEF, EuReCa and HST. The best efforts were given for protection of impact sites from post-flight contamination and physical damages in all PFAs. The contamination control, from immediately after the landing until transportation to final destinations of the components, must be properly conducted for both assessment of space environment effects and identification of particular backgrounds for subsequent analysis of impactor residues.

Ideally, once initial scanning is completed, these space flown materials should be preserved for further analyses in a clean room of a designated institution, like the NASA/ Johnson Space Centre (JSC) for LDEF and ESA/ESTEC for EuReCa and HST SCA. Those samples should be made available to scientific communities upon research proposals, which is a similar system as the existing scheme of the Antarctic meteorite collection at the National Institute of Polar Research, Tokyo, Japan. This archive system makes easier for analytical scientists to study newly retrieved space borne samples in a timely fashion. For instance, Energy Dispersive X-ray Spectroscopy (EDX), Secondary Ion Mass Spectroscopy (SIMS) and other mass spectrometers examine elemental composition of residues so that origin of impactors can be determined. However, this is only possible for non-reflight components and agreements have to be made by agencies that possess the exposed components (e.g. ISAS, NASDA and USEF in the case of SFU) prior to their deintegration.

After the landing to the NASA/KSC on 20 January 1996, the first "quick look" was conducted at KSC's Orbiter Processing Facility (OPF). Two weeks after the landing, the spacecraft was transferred to the Astrotech Space Operations (ASO) facility near KSC where we performed (1) global visual inspection, (2) photographic and co-ordinate documentation of impacts, and (3) contamination wiping and witness plate mounting in parallel to the preparation of the shipment to Japan.

Once the spacecraft returned to Japan in April, selected areas of all the faces, namely peripheral, Sun-pointing and anti-Sun faces, were visually inspected and the first impact flux measurement was made at the MELCO Kamakura Works. After the deintegration of the spacecraft in May, the M&D IIG members (Hajime Yano of ISAS, Seishiro Kibe, Sunil P. Deshpande and Michael J. Neish of the National Aerospace Laboratory [NAL]) continued further inspections of each component and payload instrument at respective manufacturers.

8-2. Objectives and Equipment at NASA/KSC

As the SFU spacecraft is designed to be re-flown several times (despite no funding guaranteed for subsequent flights at present), this first PFA had to be planned carefully. The initial PFA plan focused on the SAPs as the top priority, because they constituted about 2/3 of the total surface area of the satellite for direct comparison of dust impact flux on solar cell arrays with EuReCa and HST. Unfortunately this was not possible, owing to the unanticipated loss of both of these paddles. So the attention has shifted more to directional flux variation and chemical analysis of impactor residues on the EFFU and PLU MLI and Teflon radiators as well as the surfaces of other payload instruments.

After the SFU Project accepted the recommendation of the SFU-PFA activities submitted by the M&D IIG, the first quick look on "best effort" basis was carefully conducted and photographed by Yukio Shimizu of ISAS (SFU Project) at NASA/KSC within the first two weeks after the shuttle landing, for impact signatures and surface degradation. From the past experiences with LDEF, EuReCa and HST, the M&D IIG knew that post-flight contamination could spoil morphological and chemical analyses of impact sites and 1 atm of atmosphere could react with and develop further surface discoloration and degradation, the M&D IIG issued several instructions the post-landing operation team to minimise such drawbacks.

The first visual inspection of surface condition was conducted at NASA/KSC OPF. A special atten-

tion was given to components (e.g. trunnion pins) that must be touched and mechanically grabbed for unloading the spacecraft from the shuttle cargo bay and further transportation to the ASO such that some impact sites might have been severely damaged. The second and third eye observations were also conducted at the NASA/KSC Vertical Processing Facility (VPF) and the ASO Non-Hazardous Bay (NHB), respectively. For all the three inspections, a Nikon F4 camera and a Nikon SB-24 strobe light were used with a Nikon AF Zoom Nikkor 35–70 mm / F2.8D and Nikkor 60 mm / F2.8D lenses. Fuji and Kodak ISO 400 speed 35 mm colour negative films were used. Still images were mostly developed by NASA personnel.

8-3. Observations

Table 6 summarises the condition of these three quick looks. The three inspections proved that there was notable "Sun burn" on both Al Kapton MLIs and Ag Teflon radiators (alternatively called the "Second Surface Mirrors (SSM)), on any parts of the Sun face (-X) with a clear shielding effect by other components between the surfaces and the Sun. The Al Kapton MLI often discoloured from a bright shiny gold to a darker, less reflective sand-blasted colour while the Ag Teflon radiators became milky white colours. Also, erosions of black painted surface of the FRGF and the white painted surface of the 2D/HV plates were highly notable. A large impact site was visible on the EFFU -X Ag Teflon radiator even from a distance at the NASA/KSC VPF.

Inspections	Date (Duration*)	Place	Comments
No. 1	25/01/96 (~3.5 hours) PL =+5 days	NASA/KSC/OPF (SFU in shuttle cargo bay)	Hydrazine fuel remained in the shuttle and SFU. photographed using a strobe light outside a 3 m limit from the cargo bay.
No. 2	29/01/96 (~4 hours) PL =+9 days	NASA/KSC/VPF (SFU moved to PTRD)	Hydrazine fuel remained in SFU. Flash photography permitted.
No. 3	30/01/96 (~6 hours) PL = +10 days	ASO/NHB (SFU moved to ASO)	SFU rotated from the shuttle configuration (peripheral faces top) to the H-II configuration (Sun face top). Hydrazine fuel remained in the SFU. Flash photography prohibited because of Hydrazine safety.

Table 6 Summary of preliminary "quick looks". * = Duration includes other activities than impact search. PL = Post landing time.

The peripheral faces looked fresher than the Sun face but Sun burns were found on the EPEX boron nitride nozzle except where the MLI created shadows. Several laser reflectors were missing, possibly due to degradation of adhesives in space. No contamination nor large craters were found on the trunnion pins. A large number of ring featured impact craters, as predicted from the LDEF experience, were recognised on the Al Teflon radiators because of 5–10 times larger size of the rings (Dm) than the central pit craters (Dp). Large parts of the IRTS thermal insulators were severely torn from their stitching edges. One of the largest impact damages (Dm = 13.4 mm) was found on the side surface of the IRTS telescope body. Many small dentritic patterns were found on the inside surface of IRTS shade (see the later section).

On the anti-Sun face (+X), a colour difference between the A-system and the B-system of the Orbit Change Thrusters (OCT) was found. Inner surface of the A-system thruster nozzles turned black while that of the B-system thruster nozzles was only slightly discoloured. This might be because the A-system was used more frequently than the B-system.

9. DETAILED INSPECTION AND CONTAMINATION ANALYSIS AT ASO

9-1. Objectives

Past experience has demonstrated that contamination can be a significant factor in whether a spacecraft or satellite can successfully meet its mission objectives. The presence of contamination on a spacecraft is not necessarily synonymous with total failure of a mission, but is more frequently identified as a source of system degradation or malfunction. Contamination will be a continuing problem with future vehicles, especially those employing sophisticated electro-optics, those cooled to cryogenic temperatures or those scheduled for long lifetimes in space. Contamination can alter the power output of solar cells, distort images due to altered transmission of optical components, and degrade the reflectance and emittance of thermal control surfaces and coatings. Careful attention to contamination control is necessary to maintain maximum performance and data accuracy.

The major sources of contamination for any satellites are ground testing and operations; launch, ascent, and deployment, outgassing of detrimental materials in vacuum, impingement of thruster effluents, venting, interaction with the radiation environment, and release of particles. The key issues in contamination control are material selection and pre-flight conditioning, proper configuration and subsystem design, and initial contamination budget in assembly, testing, and maintenance procedures of satellites.

Any terrestrial or human contamination of these surfaces can seriously disrupt the chemical analysis. Some contamination is unavoidable, but by precise monitoring procedures and careful handling, their effects can be eliminated. Thus, post-flight contamination control and monitoring are important in order to avoid soiling space-exposed surfaces of the SFU during post landing operations at NASA/KSC and ASO and not to confuse subsequent chemical analysis of impact sites with the contamination.

There have been a number of reusable satellites used at ASO, and many of the post-landing operations do not require tight contamination control within the facility. Thus it was important to pay special attention to minimising further contamination at ASO. The M&D IIG suggested all the post flight operation team in Florida to always use powder-free Latex gloves when handling spaceflight hardware. Also they instructed that any spaceflight hardware to be removed should be placed face-up on a clean table that was covered with either Kapton or a non-volatile residue-transferring surface covering, such as 3M (Scotch)-2100. When these should not be available, then the table surface was thoroughly wiped with propane-1-ol. On 15–20 February 1996 (3 working days), about a month after the shuttle landing, the detailed visual inspections and contamination analysis activities were conducted at ASO by Carl R. Maag of T&M Engineering, Deshpande (NAL) and Yano (ISAS), all of who represented the M&D IIG of the JSASS and had previous PFA experiences with LDEF, EuReCa and HST. The main goal was to determine the source of any observed deposits.

9-2. Detailed Visual Inspections

At this stage, the spacecraft was in the H-II configuration and accessible to most of the parts for close inspection and for impact photographic survey except the central part of the EFFU, SEM (covered with glass hoods), OCT MLI, membranes of 2D/HV, the Sun face of the IRTS and some other small parts shielded by its complex geometry. A Canon A-1 camera with 28–135 mm zoom lens was used in conjunction with Fuji Chrome ASA 800 Super-G Plus film. A video photography was also taken in a raster fashion of some peripheral radiator surfaces to pick up impact sites. Photographs of interesting features as well as impact sites were taken and logged. Access was permitted to the top deck of SFU and a limited area of the EFFU was photographed. Yet, due to the H-II orientation, only shallow angle of incidence shots were permissible. The following is a summary of the observation at ASO.

(A) Sun Face (-X): The Teflon that loosely wrapped frame structure on the spacecraft was milky white in colour. This is typically produced by a synergistic attack of AO and UV irradiation. Some signs of self-induced outgassing from within the spacecraft were recognised. Non-uni-

form brown stains appeared to emanate from unintentional vent paths. Some surfaces had a severe increase in solar absorptance.

(B) Anti-Sun Face (+X): Slight signs of outgassing from within the spacecraft were also evident on this surface. All active louvers could not be used for impact flux counts because history of their pointing directions and their total exposed time were unknown. Impact craters on the Al blades of the active louvers could only be used for chemical analysis of impactor residues. At ASO, the OCT MLI were already removed for mounting the spacecraft on the Mechanical Ground Support Equipment (MGSE).

(C) Peripheral Faces (+/-Y and +/-Z): Principally the MLIs were severely degraded by pre-flight handling. Pre-flight fingerprints were etched into the polyimide surface from exposure to the space environment. The MLI on PLU-2 near the EPEX showed signs of darkening radially outward. One concern was that the effluent from the thruster contaminated the surface and later caused darkening due to exposure to the environment or that the plasma caused the surface darkening. The IRTS shade exhibited dendritic formations within the Teflon coating. Contamination wipes (see 9.3.) were taken to determine if the tree-like structures, or "Lichtenberg patterns", were on the surface. It may be unlikely the EPEX thrust to cause discharging on the IRTS sunshade rim to form such patterns because the whole EPEX system was grounded and thus electrically in a floating potential state. This phenomenon needs further investigations. The Grapple fixture showed signs of AO/UV degradation to the grey paint, a blend of Chemglaze black paint (TT-C-542 type 2) and a Chemglaze white paint (TT-C-542 type 1). The thermal protection paint was powdering and faded. The Teflon radiator surfaces appeared free of contamination deposits. The MLIs around the radiators were also degraded by apparent pre-flight handling. The MLIs on SPLU-1 and BSU-1 showed signs of darkening.

(D) Interior: The general appearance of the interior of the spacecraft was clean and no apparent problems were noted within the structure. Some slight blue discoloration on the underside of the Teflon close-out was seen where PLU boxes attached to the central housing frame (e.g. PLU-2 to BSU-1 and BSU-1 to SPLU-1). It is most likely that these are thin film constructive-destructive interference patterns on the metalled surfaces created by the deposition of outgassing products.

9-3. Contamination Wiping

There are two methods by which to monitor contamination on the exposed surfaces: surface wiping and placing contamination witness plates. To study "space-oriented" contaminants before they blend in with terrestrial contamination, a small area of the MLI on all the faces of the spacecraft were wiped to determine any relationships between attitude dependent deposition, cross-contamination or self-induced contamination. The wipes were taken from surfaces that visibly appeared to have a deposit on the surface. Special areas of interest, that on previous spacecraft have shown signs of deposition, were also wiped. These include interfaces between MLI blankets where venting/outgassing products escape and areas around the EPEX plasma thruster. Table 7 provides a cross-reference between the surfaces and the contamination wipe identification. The wipes consisted of "opti-cloth" cotton wipe material subjected to 10 ml of Soxhlet extraction with Methylene Chloride. The wipes were moistened with a triple distilled mixture of 1-1-1 trichlorethane and ethanol. Soxhlet is unreactive and does not damage any spacecraft components and has been used on previous space shuttle orbiters, interplanetary probes and free flyers by NASA and ESA, including the OAST-Flyer, another free flyer deployed and retrieved during the STS-72 mission.

A total of 17 samples (14 solvent wipes, 2 swab samples, plus 1 control) were submitted for Fourier Transfer Infrared (FTIR) spectroscopy in order to determine relative organic non-volatile residue (NVR) distribution and NVR chemical components. The FTIR is the technique of recording the optical spectrum of a sample material that is in contact with an optically denser but transparent medium. In actual application, the denser medium is a prism which will totally internally reflect light entering at the specified angle.

When the contaminant is deposited on one of the prism surfaces, the reflectance changes as a function of wavelength and is a measure of the interaction of the evanescent wave with the sample material. The extraction solutions were allowed to evaporate onto an FTIR window. FTIR spectra were obtained from each sample extract evaporated residue.

The search in Samples 3, 8, 9 and 17 found similar spectra for ester derivatives of long chain fatty acids; stearic acid, palmitic acid and lauric acid (Fig. 19). A match was also found for "Fingerprint Oil". "Fingerprint Oil" is made up of various organic materials including the above fatty acids. To a lesser degree, Samples 1 and 5 showed the similar features.

Fig. 20 shows the results of a spectral search with Sample 6. This search found similar spectra among phthalic acid ester derivatives. This class of material is commonly used in polymer formulations as plasticisers. However, since these materials are volatile, they would not normally be used in spacecraft materials or any vacuum applications. The absorbance around 3200–2900 wave numbers suggest longer aliphatic side groups. This is consistent with species found in some gloves or in sheet polymers used as bagging materials.

The remaining sample spectra appear to be varying mixtures of these components. There was a question of possible nitrogen containing compounds contaminating MLI surfaces, especially for Samples 10, 11 and 12. Within the constraints of this sampling technique and the sensitivity of the FTIR, no N-H absorbances associated with amines or amides (around 3200 wave numbers) were observed. Accordingly, it would be reasonable to state that neither the attitude control thrusters nor the EPEX deposited contamination on the spacecraft.

In summary, results of the contamination wiping on the SFU are as follows: (1) Long chain fatty acid ester derivatives, associated with "fingerprint oil" were found on Samples 3, 8, 9 and 17, and possibly on Samples 1, 2 and 5. (2) Two types of phthalic acid ester derivatives were found on the remainder

Sample	Location	Position	Wiped Area (cm^2)*
1	BSU-2	+X lower radiator (Ag Teflon)	40
2	BSU-2	Peripheral side radiator (Ag Teflon)	100
3	EFFU	Top deck, Left hand corner (Ag Teflon)	100
4	SPLU-2	Peripheral side MLI	100
5	PLU-4	Peripheral side radiator (Ag Teflon)	100
6	PLU-1	Peripheral side radiator (Ag Teflon)	100
7	Control	Control	N/A
8	SPLU-1	Peripheral side MLI	50
9	BSU-1	Peripheral side upper MLI	60
10	PLU-2	Peripheral side MLI [15 cm from EPEX CL; ~225° vector]	100
11	PLU-2	Peripheral side MLI [30 cm from EPEX CL; ~225° vector]	100
12	Near +X thruster	MLI on lower IRTS segment	40
13_s	IRTS	Outside edge of sunshade along "Lichtenberg pattern" (Ag Teflon)	10
14	-X top deck tank	Near 2D/HV Right hand top surface (Ag Teflon)	40
15	2D/HV	Lower expansion plate facing -X direction, Left hand corner (Ag Teflon)	100
16_s	PLU-1	Small droplet (Ag Teflon)	2
17	EFFU	Top deck along sample edge (Ag Teflon)	275

Table 7 Location of contamination wipes taken on SFU. * = approximate area (±5%); s = swab.

of the samples. (3) These phthalic acid ester derivatives were also found on the swabs. (4) No obvious nitrogen-hydrogen containing compounds were found in the wipe extracts. (5) No trace of aromaticity (i.e., species containing aromatic hydrocarbons) or silicones were found in the wipe extracts.

9-4. Contamination Witness Plates

It is known that the LDEF and EuReCa both suffered terrestrial contamination during their PFAs at NASA/KSC and ASO; the SFU would not be an exception. Thus contamination monitors (each consisting of flat plates with dimensions of 210 mm x 30 mm x 10 mm) were installed around the SFU and MGSE to observe the molecular deposition and particle fallout that occurred during the de-servicing period in the ASO Hazardous Processing Facility (HPF) after Hydrazine de-servicing. The second set was placed in the SFU shipping container to monitor molecular deposition and particle fallout during the shipping of SFU from ASO back to the MELCO Kamakura Works in Japan.

On each plate, three different specimens among the following were mounted: FTIR/IRE (Internal Reflection Element) to determine the species of any deposits; gold/copper (Au/Cu) slug for SEM analysis; black glass mirror for BRDF measurements; VUV mirror for determining molecular contamination effects; gridded particle catcher for collecting and sizing particles; and/or double-sided, flight quality, acrylic tape for catching and trapping all particles.

Three monitors were placed in three different locations in the ASO HPF on 15 February 1996 and removed on 20 February 1996. Monitor 1A was used to measure particle fallout near the SFU. Monitor

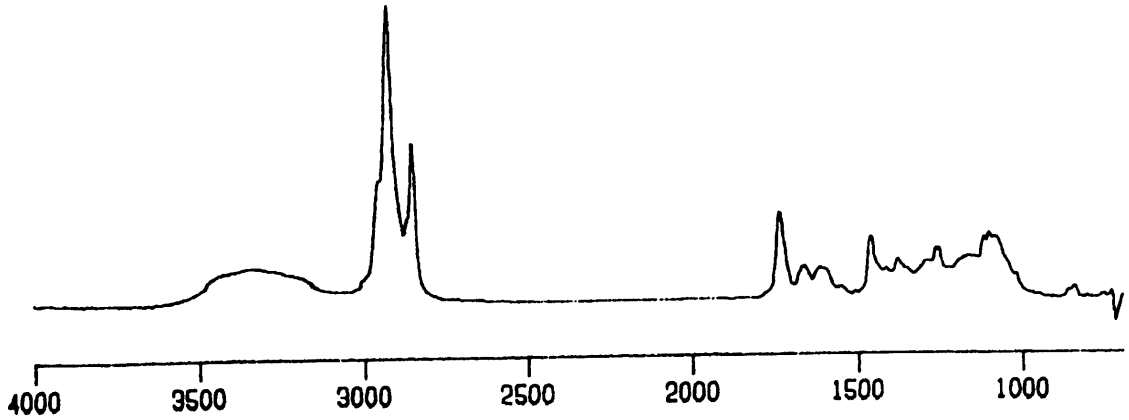

Fig. 19 FTIR spectrum of contamination wipe on the SFU Kapton determined as "fingerprint oil" (unit: wave number)

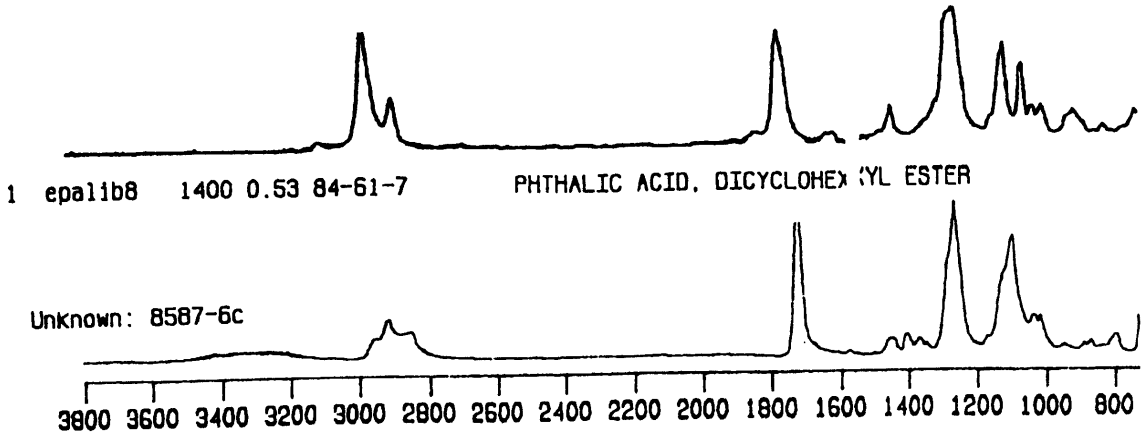

Fig. 20 FTIR spectra of phthalic acid (above) and contamination wipe on the SFU Teflon (below) (unit: wave number)

2A was used to measure particle fallout in the ASO HPF facility. Monitor 3A was used to measure molecular species and particle fallout near the SFU. Table 8 lists the monitors and position within the ASO facility. These monitors have been returned to the M & D IIG and are awaiting analysis.

Three nearly identical monitors were placed in three locations within the SFU shipping container on 20 February 1996 and were removed and covered at MELCO by the M&D IIG on 5 April right after the arrival in Japan. Monitors 1C and 2C were used to measure particle fallout while monitor 3C was used to measure molecular species (NVR) and particle fallout. Table 9 lists the monitors and location within the SFU shipping container.

Monitor	Location	Description	Approx. Area (cm^2)
1A	SFU MGSE support dolly Under BSU-2 segment	Flat surface with Scotch 3M Y-966 double sided acrylic tape	100
2A	ASO HPF Near North wall	Flat surface with gridded square	100
3A	SFU MGSE support dolly Under PLU-2	Passive contamination monitor containing FTIR IRE, Au/Cu slug, gridded cellulose disc and black glass mirror	54

Table 8 ASO facility contamination monitors

Monitor	Location	Description	Approx. Area (cm^2)
1C	SFU MGSE shipping dolly Under BSU-2 segment	Flat surface with Scotch 3M Y-966 double sided acrylic tape	100
2C	SFU MGSE shipping dolly Under PLU-1 segment	Flat surface with gridded square	100
3C	SFU MGSE shipping dolly Under PLU-2	Passive contamination monitor containing two VUV mirrors and black mirror, stainless steel slug	54

Table 9 SFU shipping container contamination monitors

10. MELCO IMPACT SURVEY CAMPAIGN AND FURTHER STUDIES BY COMPONENTS

10-1. MELCO Impact Survey Campaign

The spacecraft was safely returned first to the Tokyo Bay and then to the MELCO Kamakura Works on 4 April 1996. The contamination monitoring plates were retrieved by Deshpande, Neish and Yano on the next day. On 11 April 1996, with a firm technical support from MELCO personnel, a total of 10 members of the M&D IIG from ISAS, NAL, NASDA, Tokyo Institute of Technology, IHI, Nissan and Toshiba (for individual names, see Table 11) conducted a full day visual inspection for the first flux derivation. There, selected areas of both MLI and Teflon radiators on each peripheral face were inspected with magnifier lenses by four teams of two members each. The Sun face was not accessible except the limited areas of the IRTS body. All the Teflon radiator surfaces on the anti-Sun face were also visually inspected by another member and photographed by professional photographers from ISAS. Some large or interesting impact sites (e.g. a crater on a stainless steel bolt, inclined impact "windows", penetrations on Velcro tapes, etc.) were also revisited and taken images. The initial results were presented at the next day's press release by one of the authors (KK). Overall average impact flux above the detection limits of both MLI (Dh) and Teflon radiators (Dm) at that point was ~1×10^{-6} (m^{-2} s^{-1}), which was consistent with Fmax > 100

Components	Affiliates	Materials	Total Impacts	MLI Area (m^2)	MLI Impacts	Teflon Area (m^2)	Teflon Impacts	Other Materials	Impacts	Comments
Scuff Plates (x4)	NISSAN	Painted Al	7					Painted Al	7	Up-1=2,Low-1=4,Up-2=0,Low-2=1
Trannion Pins (x4)	NISSAN	Exposed Al	1					Exposed Al	1	
Main Structure MLI	NISSAN	MLI	14	N/M	14					
Grapple Plate	NASA	Painted Al	2					Painted Al	2	
OCT MLI	NISSAN	MLI	2	N/M	2					
BSU-1 Peripheral	MELCO	MLI/Tef	9	0.952	3	0.585	6			
BSU-1 Anti-Sun	MELCO	MLI/Tef	6	N/M	3	N/M	3			Passive Louvre Tef Scanned All
BSU-2 Peripheral	MELCO	MLI/Tef	6	0.565	5	0.24	1			
BSU-2 Anti-Sun	MELCO	MLI/Tef	6	N/M	0	N/M	6			Passive Louvre Tef Scanned All
PLU-2 (EPEX) Peripheral	ISAS/MELCO	MLI	51	1.58	51					
PLU-2 (EPEX) Anti-Sun	ISAS/MELCO	MLI/Tef	0	N/M	0					
SEM	DENSO	MLI/P Al/Tef Al	18	N/M	17			Painted Al	1	on Pole
			5					Teflon Tape Al	5	Sun face; MLI impacts include 2 on RFC
SHANT (x4)	TOSHIBA	P Al/Tef Al	1					Painted Al	1	
			5					Teflon Tape Al	5	
RCS Tank MLI	MHI	MLI	1	N/M	1			Sun Face		
PLU-1 Peripheral	IHI	MLI/Tef	18	0.1967	5	0.399	13			
PLU-1 Anti-Sun	IHI	MLI/Tef	2	N/M	0	N/M	2			Only around active louvre
PLU-4 Peripheral	IHI	MLI/Tef	17	0.0225	4	0.4717	13			
PLU-4 Anti-Sun	IHI	MLI/Tef	0	N/M	0					
SPLU-1 Peripheral	HITACHI	MLI/Tef	10	0.4427	7	0.09	3			
SPLU-1 Anti-Sun	HITACHI	MLI/Tef	11	N/M	0	0.499	11			
SPLU-2 (MEX/BIO) Peripheral	ISAS	MLI/Tef	11	0.288	11					
SPLU-2 (MEX/BIO) Anti-Sun	ISAS	MLI/Tef	1	N/M	1	N/M	0			
IRTS	ISAS	Ag MLI/Tef Al	3	N/M	1			Teflon Tape Al	2	Body and Shade
2D/HV	TOSHIBA	P Al/Kap Film	6					Painted Al	6	Base=1.Front=3,Rear=2
SPDP	MEISEI	MLI/ Tef Al	1	N/M	1			Teflon Tape Al		Dh =1mm/
EFFU Sun	IHI	Tef	28			2.19	28			
EFFU Peripheral (+Y)	IHI	MLI	19	1.554	19					
EFFU Peripheral (-Z)	IHI	MLI	14	1.554	14					
EFFU Peripheral (+Z)	IHI	MLI	36	1.554	36					
EFFU Peripheral (-Y)	IHI	MLI	26	1.554	26					
TOTAL			337	10.2629	221	4.4747	86	0	30	

Table 10 Summary of the combined results of the early SFU visual inspections in the first 6 months after the retrieval. Keys: N/M = Not measured yet; P = painted; Tef = Teflon or Teflon taped; Kap = Kapton.

μm (Fmax = marginal perforation thickness of Al 1100–0 alloy plates) of the LDEF 6 point average flux, Dco > 500 μm (Dco = conchoidal fracture zone diameter) of the EuReCa solar cells, and Dco > 700 μm of the HST solar cells. The further details of the results are summarised in Table 10.

10-2. Protection of Impact Sites

After the MELCO campaign, the spacecraft was deintegrated and each component was returned to their respective manufacturers or PIs. Then we protected the most valuable impact sites on the SFU surfaces with simple Perspex caps. The protective covers were attached to the SFU surfaces by means of Kapton tape. The covers ensured that handling of the MLI, Teflon radiators or other components does not damage the impact sites on them (Fig. 21). In total, more than a dozens of impact sites on PLU-1 and 4, SPLU-1, IRTS and the main frame have been protected. In addition, when storing MLI blankets care was taken not to fold the blankets. Where necessary folds were made along the natural folds on the MLI edges so that deformation of the impact sites became the minimum.

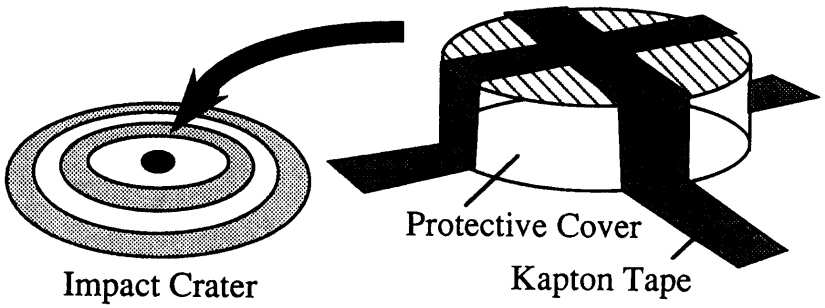

Fig. 21 A protective cover for an impact crater on the SFU surface

10-3. Detail Analyses of Specific Payloads

Thereafter the M&D IIG visited individual PIs and manufacturers for assessment of each component to identify which part to conduct detail flux measurements as well as potential candidates for chemical analyses (Table 11).

At this point, in addition to impact studies, material property evaluation (i.e. degradation, contamination build-up, etc.) drew interests of material scientists and respective manufacturers, namely Rikio Yokota of ISAS, MELCO, IHI, Nissan, etc. The SFU Project compromised that the M&D IIG should work together with the material group and avoid areas with large and valuable impacts prior to their cutting MLI and other surfaces. Therefore, assessment visits were usually made with the presence of the USEF personnel to witness the activities and mutual agreements among the SFU Project, M&D IIG and material researchers. As the results, the M&D IIG evaluated all the surfaces for levels of further scanning and analyses, except the BSU-1 and 2 Teflon radiators, which were already coffined in storage boxes by MELCO before the inspections were planned.

To reduce the handling and transit times of the detailed CCD and laser scanning, the following items were sealed in space approved bags and containers and moved from payload manufactures to a clean booth at NAL, a main site of M&D IIG scanning activities.:

(1) Al Kapton MLIs on all PLU, SPLU and BSU boxes as well as the main structure, IRTS, EFFU, SEM and SPDP

(2) Ag Teflon radiators on PLU-1 and 4 (access panels)

(3) Other surfaces including scuff plates and SHANT plates and stands

At the time of writing, the Teflon radiators of the SPLU-1 and SPLU-2 will be scanned on site of HITACHI Totsuka Works and ISAS, respectively in September–October. The BSU-1 and 2 have to be waited until they are open again for future programmes. The EFFU radiators are still kept at NASDA.

The two-Dimension High Voltage Solar Array Experiment (2D/HV) (a triangle sail of 3.84 m height

Facility	Scanned Components	Materials	Dates	M&D IIG Participants
ASO (Titusville, Florida, U.S.A.)	Whole Spacecraft with some exceptions	MLI, Teflon, Painted/Teflon Tape Al Plates	15-20/02/96	C.R.Maag, SPD, HY
MELCO (Kamakura, Kanagawa)	Whole Spacecraft with some exceptions	MLI, Teflon, Painted/Teflon Tape Al Plates	11/04/96	HY, SPD, MJN, A.Fujiwara, T.Takano, H.Yurimoto, A.Miyoshi, N.Yoshioka, Y.Kitazawa, M.Tanaka
IHI (Mizuho, Tokyo)	EFFU	MLI, Teflon	22/05/96	Y.Kitazawa, R.Amagata, HY (observer)
Hitachi (Totsuka, Kanagawa)	SPLU-1	MLI, Teflon	10/06/96	MJN, SPD, HY
MELCO (Kamakura, Kanagawa)	BSU-1 & 2	MLI	10/06/96	SK, HY
Nissan (Ogikubo, Tokyo)	Scuff Plates, Main Frame MLI, OCT MLI	MLI, Painted Al plates	13/06/96	HY
Toshiba (Komukai, Kanagawa)	SHANT	Painted Al Plates, Teflon Tape Al Plates	13/06/96	HY
IHI (Mizuho, Tokyo)	PLU-1 & 4	MLI, Teflon	14/06/96	SK, SPD, MJN, HY
ISAS (Sagamihara, Kanagawa)	PLU-2 (EPEX) & SPLU-2 (MEX/BIO)	MLI, Teflon	17/06/96	HY
DENSO (Nukata, Aichi)	SEM	MLI, Teflon Tape Al Plates, Painted Al Plates	20/06/96	HY, MJN
Meisei (Tsukuba, Ibaraki)	SPDP	MLI, Teflon Tape Al Plates	21/06/96	SK, SPD
ISAS (Sagamihara, Kanagawa)	IRTS	MLI, Teflon Tape Al Plates, Exposed Al Plates	28/06/96	HY

Table 11 Summary of component inspections. Keys: SK = Seishiro Kibe, SPD = Sunil P. Deshpande, MJN = Michael J. Neish, HY = Hajime Yano.

x 3.62 m baseline at the full open configuration) was an engineering experiment to test deployment and folding of a flexible membrane structure called the "Miura-ori" folding and the feasibility of high voltage solar cells. It was opened and folded in different time of the mission. Although its cumulative exposed time was as short as a few orbits (thus the number of impacts is also expected to be small), its sail had a unique time resolution (time of arrival) with known orbital and attitude parameters of the spacecraft at times of impacts. These can give some clues of origins of impacted meteoroids (i.e. streams vs. sporadic) as well as a lower limit on the impact flux, unlike any other parts of the SFU whose impact flux were all integrated in the 10-month exposure. Also its thin film sail can be examined their both sides so that exposed areas are doubled (~14.3 m^2) while the solar cell parts are the only area left that can be directly compared with those of EuReCa and HST after the loss of the main SAPs. Impacts on the 2D/HV support structure are also important for comparison with painted Al plates of LDEF and EuReCa. Thus it is

strongly suggested to conduct visual inspection and photography of impacts on the 2D/HV sail when it is opened and laser microscopy of impacts on the painted plates on site (i.e. Toshiba Keihin Works).

11.COMBINED RESULTS OF PRELIMINARY PFA

11-1. Impact Data Summary

Through these initial visual inspections with magnification lenses (x3–6) 337 impact features were logged in nearly 18 m^2 of the various material surfaces. Three largest impact damages were (1) a crater on the Teflon coated Al body of the IR telescope with Dc = 2.5 mm and Dm = 13.4 mm (Fig. 22); (2) a penetration on the edge of the MLI around shade of the IR telescope with Dh = 4.5 mm and torn parts extending > 20 mm (Fig. 23); and (3) a crater on the Ag Teflon radiator on the Sun face EFFU with Dp = 500 μm, Dr = 2.5 mm, Dc = 4 mm and Dm = 10.5 mm (Fig. 24).

On the Kapton MLI, whose top layer was 50-μm thick, 221 impact penetrations were counted in the area of 10.3 m^2 with the detection limit of Dh = ~200 μm. Although most of them were complete penetration holes with developed lips, some notable features were evidences of inclined impacts and embedded impactors in Velcro tapes. At least 8 impacts showed not only elongated holes but also transparent "windows" at the down range of their impacts, due to vaporisation of Al coating by ejecta plume from subsequent layers after the primary penetration (Fig. 25). Also at least 12 impacts occurred on the top of Velcro tapes, which connected segments of the MLI each other, and fragments of destroyed layers and

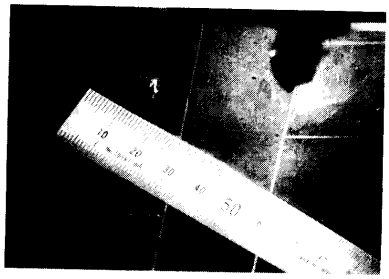

Fig. 22 Crater on Al telescope body covered with Kapton tape for IRTS [Sun (-X) face]; Dc = ~2.5 mm, Dm = ~13.4 mm (Photo courtesy: ISAS)

Fig. 23 Penetration on edge of MLI around the Al telescope shade for IRTS [Peripheral face]; Dh = ~4.5 mm, Torn part extended >20 mm (Photo courtesy: ISAS)

Fig. 24 Crater on Ag Teflon radiator of the EFFU on Sun (-X) face; Dp = ~500 μm, Dr = ~2.5 mm, Dc = ~4 mm, Dm = ~10.5 mm (Photo courtesy: ISAS)

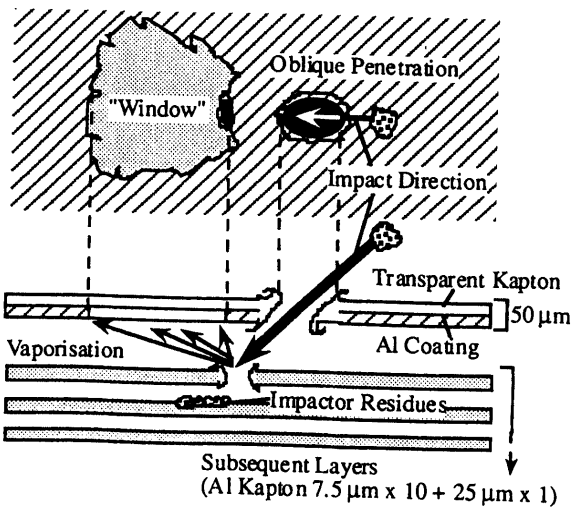

Fig. 25 (Above) Inclined impact penetration on Al Kapton MLI on the peripheral face of PLU-2 [EPEX]; Dh = ~500 μm; cf. Vent hole =~500 μm; Impact direction: ~40° from the Sun face (Photo courtesy: ISAS). (Right) Mechanism of the "window" formation by an inclined impact.

possible impactor remnants were captured intact, promising chemical analysis of the residues to conclude their origins (Fig. 26). As the SFU MLI has the twelve layered structure (50 μm x 1, 7.5 μm x 10 and 25 μm x 1), it generally works as an effective "foil stack capture cell". Thus together with the Velcro impacts, the higher survivability of impactor remnants are expected than those on thick metal and glass plates.

As for the Ag Teflon radiators, the 4.5 m^2 scanned area marked 86 impact craters with shock wave induced ring features, as previously reported for surfaces of the UHCRE of LDEF by Mullen and McDonnell (1994), above the detection limit of Dm = ~700 μm. About half of those craters exhibited streaks of ejecta, again implying their impact directions to some degree. Other components including painted Al plates and Teflon coated Al plates also counted 30 micro-craters and they are able to be directly compared morphologically with impact data on the Al plates of LDEF and EuReCa.

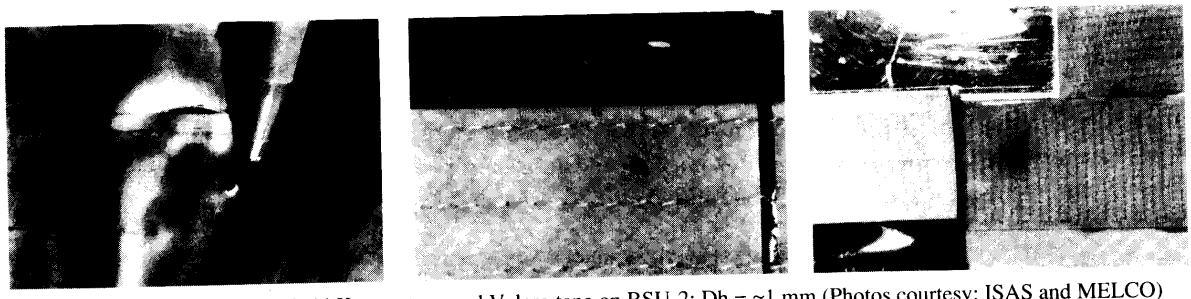

Fig. 26 Penetration through Al Kapton tape and Velcro tape on BSU-2; Dh = ~1 mm (Photos courtesy: ISAS and MELCO)

11-2. Preliminary Impact Flux Derivation

Fig. 27 illustrates the flux variation at the visual detection limit on both the Kapton MLI and Teflon radiators with respect to peripheral angles around the Sun-spacecraft line. For the MLI impacts, the PLU-4 surface being 22.5° off to the north of the +Z face, the direction of the Earth's apex, raised the peak

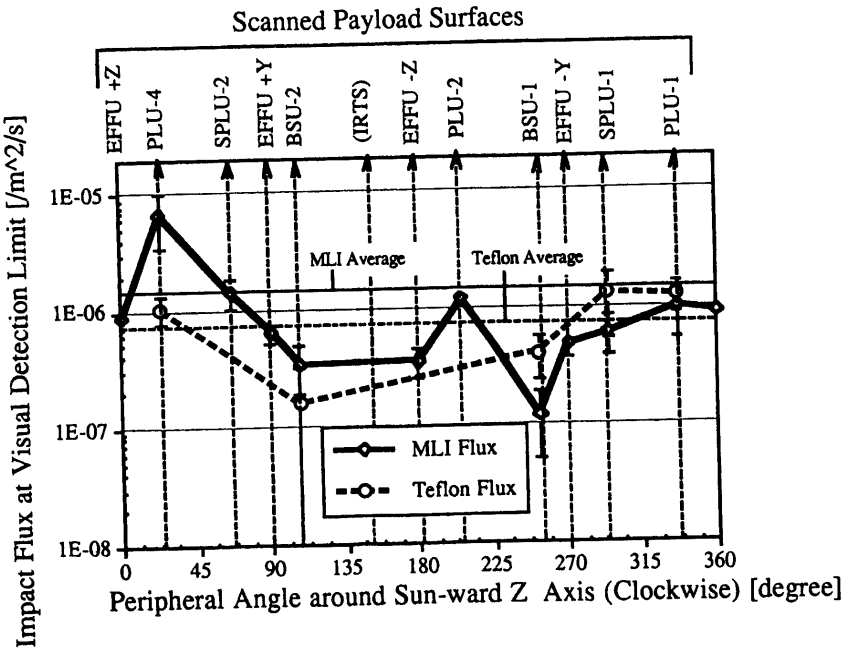

Fig. 27 Peripheral angular distribution of impact flux on the SFU around the Sun-spacecraft line. Detection limit sizes: Dh ≈ 200 μm for MLI; Dm ≈ 700 μm for Teflon.

while the lowest flux occurred on at the BSU-1 surface at 65.5° off to the south of the anti-apex face. Their average flux difference is nearly a factor of 50. The Teflon flux was less heterogeneous but the apex surfaces (PLU-1 and 4 and SPLU-1) exceeded the anti-apex surfaces (BSU-1 and 2) by a factor of 5 at maximum. These results are not inconsistent with the impact data of EuReCa reported by UniSpace Kent (1994) indicating a flux enhancement at the Earth's apex. However the attention must be drawn to the facts that this SFU data set is from only selected area of each face (thus varying the error range) and has not incorporated with local shielding effects by the spacecraft geometry, including the SAPs at 90° (+Y) and 270° (-Y). These corrections will be carried out before drawing any further interpretations on this matter.

As for the Sun face to anti-Sun face flux ratio of the Teflon impacts, the anti-Sun face received 1.7 times more flux than the Sun face with no local shielding effect while the scanned area of the anti-Sun face (0.50 m^2) was 4.4 times smaller than that on the Sun face (2.19 m^2). Even if this is not observational artefact, β-meteoroids (d < 1 μm) from the solar direction would not increase the observed impact flux due to the larger detection limit. Plausible causes of this anti-Sun bias of meteoroids are still under the investigation; yet there are several possible contributors (whether minor or major) including (1) a combination of the Poynting-Robertson effect of relatively large (i.e. 10–100 μm) meteoroids (spiralling into the Sun and intersecting the Earth's orbit from outside), (2) anti-Earth's apex enhancement of circumsolar asteroidal dust near 1 AU (Dermott *et al*, 1994), and (3) a stronger Anti-Helion component of fast-moving radar meteor observation than the Helion component (Taylor, 1996). To make further comments, accurate flux measurements of smaller crater sizes and confident impact calibration efforts for the Teflon targets are vital.

11-3. Sun Face EFFU Impacts

In particular, 28 impact craters on the Sun face EFFU Ag Teflon radiator were studied their morphology. Fig. 28 shows size ratios of the various diameters of the Teflon craters. Progression of all three ratios with increasing the Dm size is recognised, except the largest impact of Dm = 10.5 mm dropping the

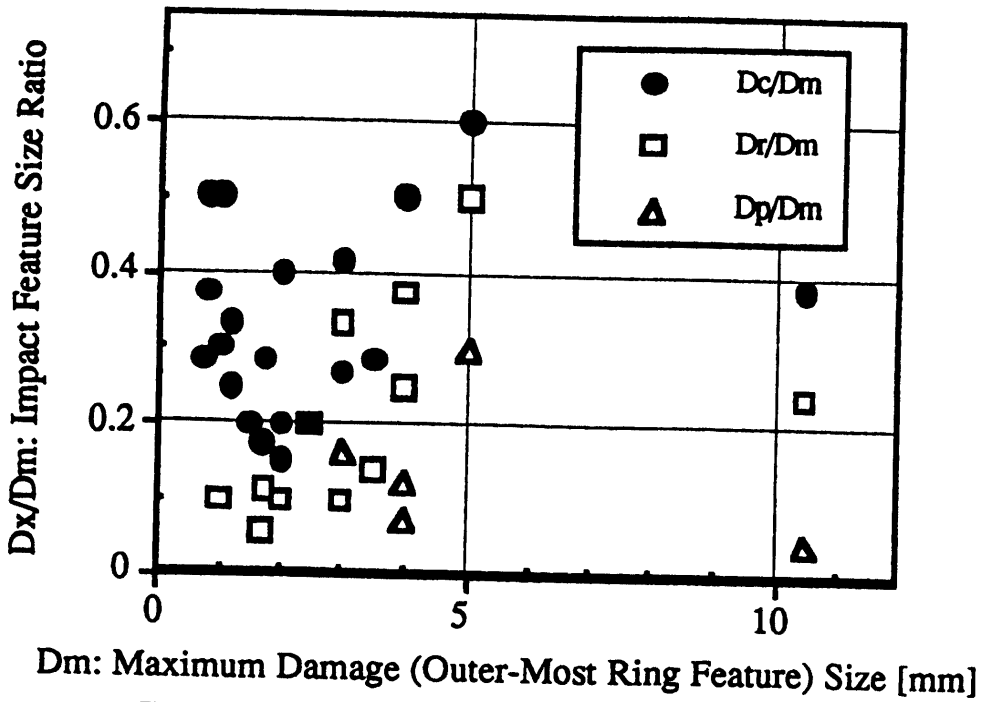

Fig. 28 Size ratios of impact features on the Sun face EFFU Teflon radiator.

ratios significantly. This may suggest that shock wave propagation rings get larger as Dp, Dr and Dc develop (= impact energy become higher) until the radiator surface is completely penetrated and a large portion of the impact energy is consumed to excavate the Al substrate underneath. Such impact phenomena at material boundaries were reported for impacts penetrated through solar cells and their substrates on HST by Space Applications Services (1995).

Fig. 29 shows the cumulative fluxes of crater parameters on the Sun-face EFFU Teflon with the LDEF 6 point average smoothed flux of Fmax as a reference. Note that smaller features have less dataset due to the low resolution scanning. The Dc or Dp are closer to the Fmax values and carry more direct information of impactor size than the Dm.

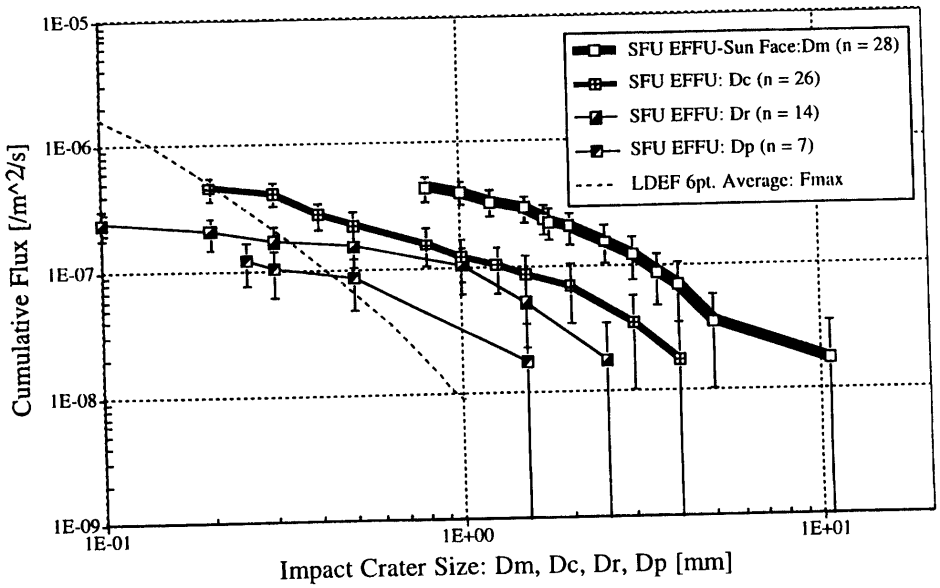

Dm = Maximum Damage (Outer-Most Ring Feature); Dc = Main Crater Diameter; Dr = Lamina Rim Diameter; Dp = Central Pit Diameter

Fig. 29 Size distribution of large impact features on the Sun face Ag Teflon radiator of the SFU

11-4. Direct Comparison with LDEF, EuReCa and HST

Comprehensive comparison of different spacecraft with different target materials are subject to accurate impact calibrations. Such efforts for Al alloy and glass have been addressed by several researchers but there are a lot to be done for Teflon and Kapton. Meanwhile, we are still able to compare the size distribution index (α = graph slope) of the cumulative flux curves of the impact features on Al (LDEF surfaces and EuReCa TiCCE mesh support), glass (EuReCa and HST solar cells) and Teflon (SFU EFFU) (Fig. 30).

We chose Fmax for LDEF and EuReCa TiCCE as a transformed parameter from Dh and Dc while the solar cell impacts were studied their conchoidal fracture diameter (Dco) and Dm for the EFFU rather than Dp because these were all the parameters used for their initial impact search. The α of EFFU except the largest one is in a good agreement with the EuReCa TiCCE in Fmax = 0.03–0.2 mm and the EuReCa and HST solar cells in Dco = 0.2–1 mm. The LDEF Fmax also agrees with the EFFU in a narrower range of 0.03–0.1 mm. Yano (1995) converted the EuReCa and HST solar cells data to Fmax and showed that the impact fluxes of the three spacecraft agreed with each other within the average error range of 1σ in 0.2–1 mm of Fmax. The same effort including cross calibration impact experiments for the Kapton and Teflon is in progress.

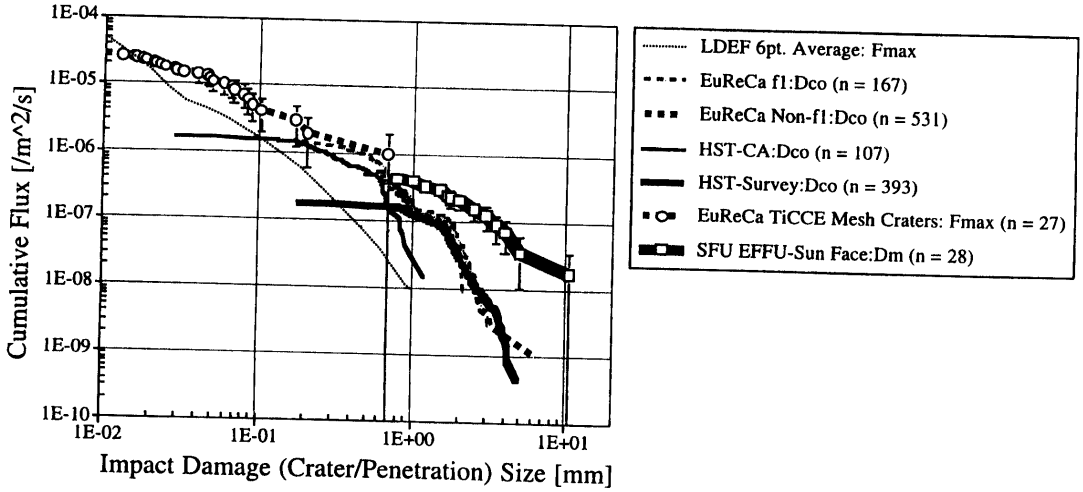

Dm = Maximum Damage Diameter (Ag Teflon)
Dco = Conchoidal Fracture Diameter (Solar Cell Glass Cover)
Fmax = Converted Values from Crater Diameter to Marginal Perforation Thickness of Al Plate

Fig. 30 SFU EFFU Ag Teflon radiator impact flux (Dm) directly compared with fluxes of LDEF 6 point average Al plates (Fmax), EuReCa TiCCE (Earth's apex/Sun face) Al mesh supports (Fmax), EuReCa and HST solar cells arrays (Dco). All the data except SFU are adapted from Yano (1995).

12. FURTHER ANALYSIS PLANS

12-1. Scanning System

If one wishes to study smaller impact features, the initial scanning system has to trade off between the smallest resolution and duration of the scanning. For non-penetrated craters, the depth to diameter ratio (P/Dc, P/Dco) is essential for establishing empirical scaling laws to derive impactor density. Yet no previous PFAs of LDEF, EuReCa and HST SCA performed depth measurements at the initial scanning. Thus the SFU-PFA should use the scanning system combining a singular colour CCD camera with multi-magnification lenses for image capture and a laser microscope for dimension measurement including crater depth profile on a three dimensional motion rig in a controlled environment (Fig. 31) (Yano *et al.*, 1996). As previously explained, detailed scanning of the MLIs, some Teflon radiators and painted Al plates will be conducted in a Class 10,000 clean booth or better at NAL, with laminar flow and with the appropriate clean room attire when in close proximity to the surfaces. Each surface shall be placed on a cleaned, covered table with a 3 axis scanning rig housing the optics for locating impact sites and measuring the features. Two systems shall be used in scanning the surfaces.:

(1) A variable magnification 10^6 pixel CCD microscope is used first to locate the impact sites in a wider field of view (lower magnification) and then to revisit the sites and take images for measurements with a finer resolution, a magnification of up to x 800. The position of these sites are logged by a computer programme with the aid of a reference origin point placed on the scanned surface.

(2) A LaserTec laser microscope is used to measure the dimension of impacts, including crater depth profile (P/Dc). The measured data are stored for subsequent analysis alongside the digital image.

Its computer system controls the movement of the rig and records all data including positions of impacts with digital images from CCD and laser microscopes. Design of the scanning table (or specimen support) depends upon how inspected surfaces can be installed (i.e. horizontally placed or vertically suspended) but the rest of the scanning system and control software can be common. Consequently, the current PFA programme will lead to the whole area scanning with higher resolution than naked eye: MLI for Dh(min) = ~200 μm and Teflon for Dm(min) = ~200 μm.

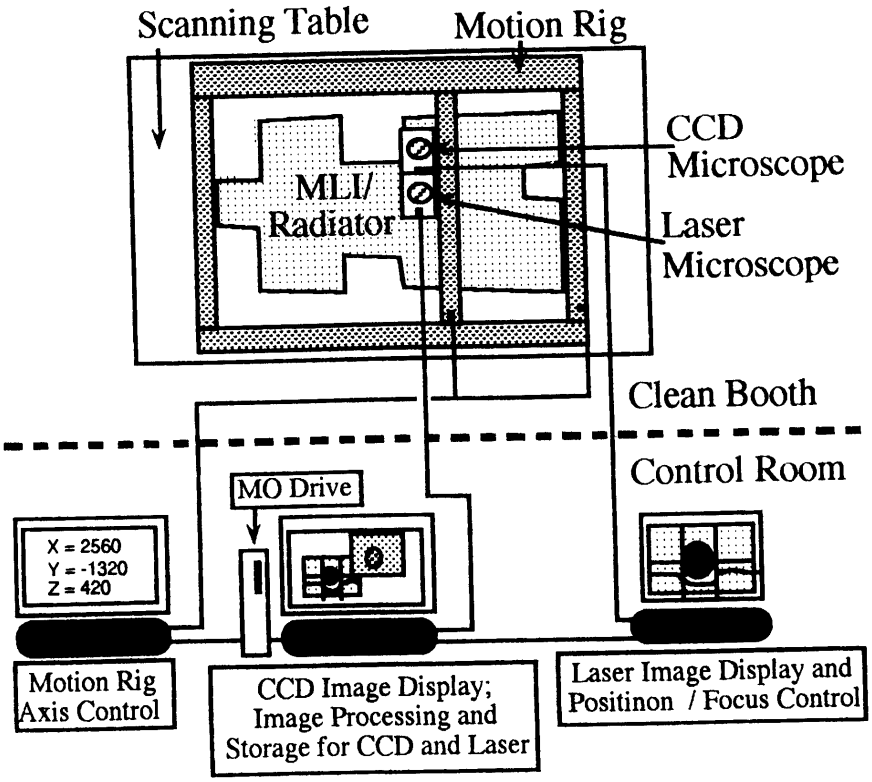

Fig. 31 SFU MLI and radiator scanning system

12-2. Chemical Analysis

Sites that warrant further analysis will in general be large impacts and those where a good chance of impactor remnants exist (e.g. impacts into MLI and Velcro tapes). These sites will be designated for chemical analysis using an SEM and associated EDX. To facilitate the chemical analysis the impact will have to be cored from the surface. This will be carried out using a proven method to ensure the integrity of the surface and layered structure. The samples will then be analysed in an SEM and qualitative elemental composition determined and any impactor residue characterised. After the initial characterisation of the residues, further analyses in terms of chemical, mineralogical, isotopic, noble gas, cosmic ray, etc. should be made possible upon request to the curation of the programme (e.g. CDPET and M+D SIG in NASA/JSC). Thus it is necessary to assign some facilities for the curatorial work soon.

12-3. Impact Progression Analysis

The surfaces of Kapton MLIs can record the progression of impacts through the multi-layers and gleam information on the impactor direction and velocity. Large impacts into MLI will be de-laminated and subsequent penetrations through each layer documented to provide data on the progression of the impact size through the layers, maximum penetration depth and possible direction.

12-4. Database Architecture

In order to study the evolution of the dust population in long time integration and comparison of impactor compositions, the data archive system must have a commonalty with the past PFAs such as LDEF (NASA/JSC), EuReCa and HST (ESA/ESTEC). In the future, digital images and spreadsheets of the SFU-PFA should be made available for file transfers via the World Wide Web like the Planetary Material Laboratory of NASA/JSC, in addition to storage in Magneto-Optical discs or recordable CDs for

physical mailing, so that the global research community can easily access to the data. This data base will serve as Japan's first contribution of the real space data that can be shared with the international meteoroid and debris community.

12-5. Hypervelocity Impact Calibration Tests

In order to derive impactors' information and compare the impact flux with metal and glass surfaces of the previous spacecraft, HVI calibration experiments for Kapton MLI and Teflon (e.g. Hörz *et al.*, 1994b) are necessary. Currently such efforts for Kapton films are in progress by using two stage light gas guns at ISAS and the University of Kent at Canterbury, U.K.

Projectiles used are Alumina (~50 μm) and glass beads (50–100 μm) accelerated by the "shot gun" technique using a newly designed split sabots (Fig. 32). At ISAS, this technique still has some improvements in the area of gun centering, projectile scattering, projectile survivability, impact flash measurement, and separation of projectile impacts from gun debris.

Once equations of state of both Kapton and Teflon are empirically established, Hydrocode (e.g. Autodyn-2D) computer simulations can be applied for higher velocity regimes than laboratory experiments.

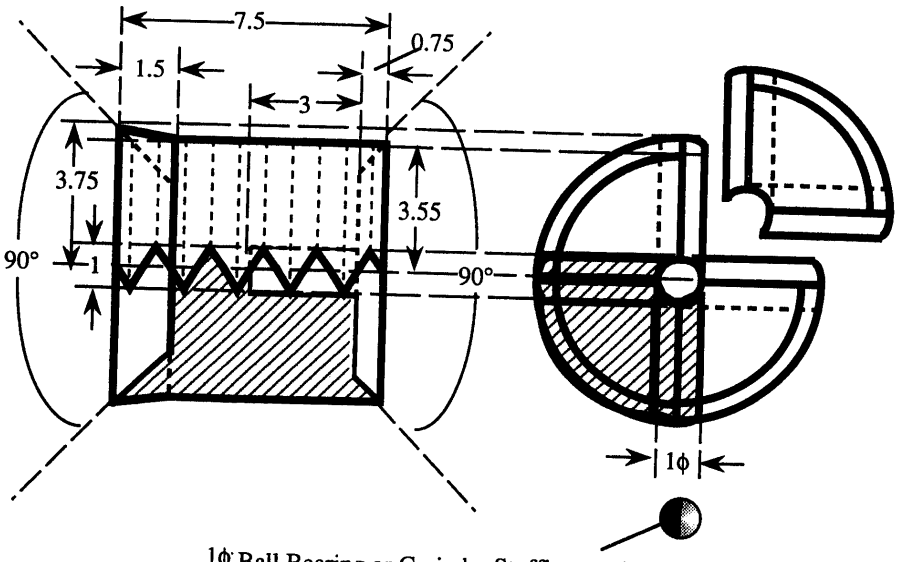

Fig. 32 Split sabot design for the ISAS light gas gun (courtesy: H.Yano)

13. FUTURE EXPERIMENT OPPORTUNITIES: SHUTTLE MISSION AND SPACE STATION ROUTINE PFA

The SFU was the first of retrievable components flown in space for the Japanese space programme. Yet in the next decade, there are more opportunities for such in-situ dust detection in the LEO. The next space-flown components to be returned to Japan will be the Manipulator Flight Demonstration (MFD) shuttle mission for the assessment of the JEM robot arm and experiments. It is currently allocated a shuttle launch in July 1997. There is an exposed pallet fixed in the orbiter cargo bay that mounts dust collectors using aerogels of 0.03 g/cm^3 density. Despite its short exposure time of ~40 hours in the apex direction and the whole mission in ~10 days, several impacts by 1–10 μm range particles (mainly apex orbital debris) are expected in ~400 cm^2 area. It will mark as the first of its kind designed and manufac-

tured in Japan. Currently calibration impact simulations, and development of subsequent extraction method are being performed by NASDA and IHI.

When the ISS becomes operational at 400 km altitude and 51.7° inclination, it is planned to exchange the Experiment Logistic Module-Exposed Section (ELM-ES) of JEM in orbit repeatedly and to be returned to the Earth. This will provide a unique opportunity for "routine" PFA of space exposed surfaces. This activity will enable to monitor the dust environment on continuous basis and refine the evolving dust flux models in the next decade. The JEM-EF also provides four fully exposed faces with respect to the Earth gravity stabilised attitude of the station (east, west, north and space) in the maximum of 10 years. In particular, the trailing and space-pointing faces are where meteoroid impacts exceed artificial debris. It also has an in-orbit service capability with its robot arm. This will allow collection modules to be exposed only to specific dust sources such as high flux meteoroid storms and newly generated debris swarms. Such dust collection and detection facility has been proposed (Yano, 1994) and the small part of the payload called Space Environment Monitoring System could be allocated for a dust collector. In addition the JEM will exchange its exposed payload pallets every 3–6 months; thus ground laboratories can regularly receive space exposed targets in that frequency (Yano *et al.*, 1996).

14. SUMMARY OF THE CURRENT RESULTS

The current impact investigation of the SFU spacecraft is in good progress and producing abundant and rather unique impact data on Kapton MLI and Teflon targets, which previously have not been studied in full extent. On the Kapton MLI, some directional information can be deduced and its capture cell structure promises a high survivability of residues for subsequent chemical analysis from EDX to SIMS. The Kapton radiators exhibited the same impact features as thermal blankets of the previous retrieved spacecraft. The peripheral flux variation is not inconsistent with the EuReCa data favouring for the Earth's apex but further analysis of geometrical effects must be incorporated. The anti-Sun face flux exceeded the Sun face by a factor of 1.7. The size distribution index of the impact maximum damages on the Sun face Teflon surface agreed with the certain size ranges of the previous spacecraft data set; yet the cross impact calibration tests amongst Al, glass and Teflon must be conducted for comparison with a unified parameter.

Detailed CCD and laser microscopic survey will yield much smaller crater/penetration size regimes than the visual inspections, including crater depth profiles. Chemical analyses on MLIs and Velcro tapes seem promising but some curatorial institutions are needed for preservation and distributions of the samples. The HVI calibration experiments for direct comparison with the past PFA data of metal and glass targets are also in progress. The data archive system has been designed to have commonalty with the previous PFAs such that the international scientific community can utilise the SFU dataset as Japan's first contribution for the meteoroid and space debris database.

ACKNOWLEDGEMENTS

The authors wish to acknowledge Hajime Yano and Susumu Sasaki of ISAS for preparation of this report and their editorial work. Yukio Shimizu of ISAS, Sunil P. Deshpande of NAL and Carl R. Maag of T&M Engineering also contributed textual and visual materials. Hitoshi Kuninaka and Kyoichiro Toki of ISAS and Masaru Okamoto of MELCO supported the PFA operation at ASO. The authors also thank the members of the SFU Project (i.e. ISAS, NASDA, NEDO/USEF) and contract manufacturers (i.e. Denso, Hitachi, IHI, Meisei, MELCO, MHI, NEC, Nissan, Toshiba) for their co-operation to conduct this activity. All the PFA activities except the earliest work at NASA/JSC have been conducted by the M&D IIG of JSASS, in which one of the authors (TY) and Seishiro Kibe of NAL lead.

REFERENCES

Carey, W.C., McDonnell, J.A.M. and Dixon, D.G.: An empirical penetration equation for thin metallic films used in capture cell techniques, Properties and Interactions of Interplanetary Dust, (*edit.*) Giese, R.H. and Lamy, P., D. Reidel Publishers, 131–136, (1985).

Dermott, S.F., Nicholson, P.D., Burns, J.A. and Houck, J.R.: Origin of solar system dustbands discovered by IRAS, *Nature*, **312**, 505–509, (1984).

Dermott, S. F., Jayaraman, Y.L., Gustafson, B.A.S. and Liou, J.C.: A circumsolar ring of asteroidal dust in resonant lock with the Earth, *Nature*, **369**, 719–723, (1994).

Divine, N., Grün, E. and Staubach, P.: Modelling the meteoroid distribution in interplanetary space and near-Earth, *Proc. First European Conf. on Space Debris*, **ESA SD-01**, 245–250, (1993).

Grün, E., Zook, H.A., Baguhl, M., Fechtig, H., Hanner, M.S., Horanyi, M., Kissel, J., Lindblad, B.A., Linkert, D., Linkert, G., Mann, I.B., McDonnell, J.A.M., Morfill, G.E., Phillips, J.L., Polanskey, C., Riemann, R., Schwehm, G., Siddique, N., Staubach, P., Svestka, J. and Taylor, A.D.: Discovery of Jovian dust streams and interstellar grains by the Ulysses spacecraft, *Nature*, **362**, 428–430, (1993).

Hörz, F., Cintala, M., Bernhard, R.P. and See, T.H.: Dimensionally scaled penetration experiments: Aluminium targets and glass projectiles 50 μm to 3.2 mm in diameter, *Int. J. Impact Engng*, **15**, No.3, 257–280, (1994a).

Hörz, F., Cintala, M., Bernhard, R.P. and See, T.H.: Penetration experiments in aluminium and Teflon targets of widely variable thickness, Analysis of Interplanetary Dust, *AIP Conf. Proc. 310*, (*edit.*) Zolensky, M.E., Wilkson, T.L., Rietmeijer, F.J., and Flynn, G.L., AIP Press, 329–343, (1994b).

Jehn, R.: Private communication, ESA/ESOC, Darmstadt, Germany, (1995).

Johnson, N.L. and McKnight, D.S.: Artificial Space Debris, Orbit Book Company, (1987).

Kessler, D.J.: Collisional cascading: The limits of population growth in Low Earth Orbit, *Adv. in Space Res.*, **11**, No.12, 63–66, (1991).

McDonnell, J.A.M.: Microparticle studies by space instrumentation, Cosmic Dust, (*edit.*) McDonnell, J.A.M., John Wiley & Sons, 337–426, (1978).

Mullen, S. and McDonnell, J.A.M.: LDEF Particulate Environment Characterisation: Final Report, ESA/ESTEC/MAF Contract Report, **Contract No 110745**, Noordwijk, the Netherlands, (1994).

National Research Council USA - Committee on Space Debris / Aeronautics and Space Engineering Board / Commission on Engineering and Technical Systems, Orbital Debris: A Technical Assessment, National Academy Press, (1995).

Reach, W. T., Franz, B.A., Weiland, J.L., Hauser, M.G., Kelsall, T.N., Wright, E.L., Rawley, G., Stemwadel, S.W. and Spiesman, W.J.: Observational confirmation of a circumsolar dust ring by the COBE satellite, *Nature*, **374**, 521–523, (1995).

See, T.H., Allbrooks, M., Atkinson, D., Simon, C. and Zolensky, M.: Meteoroid and Debris Impact Features Documented on the Long Duration Exposure Facility: A Preliminary Report, **NASA/JSC Publ. No. 24608,** Planetary Science Branch Publication No. 84, NASA/JSC, Houston, USA, (1990).

Space Applications Services (Carey, W.C.), Unispace Kent (McDonnell, J.A.M. and Zarnecki, J.C.), Mare Crisium (Stevenson, T.J. and Deshpande, S.P.) and ONERA/CERTS-DERTS (Mandeville, J-C): (edit.) Carey, W.C., Prepared by Carey, W.C., Fowler, M., Griffiths, A.D., McDonnell, J.A.M., Mandeville, J-C., Nichol, K., Quant, A., Shrine, N., Stevenson, S.J., Taylor, E.A. and Yano, H.: Hubble Space Telescope Micrometeoroid and Debris Post Flight Analysis, ESA/ESTEC Contract Report, **Contract No: 10830/94/NL/JG,** Noordwijk, the Netherlands, (1995).

Taylor, A.D., Baggaley, W.J. and Steel, D.I.: Discovery of interstellar dust entering Earth's atmosphere, *Nature*, **380**, 323–325, (1996).

Taylor, A.D.: Radiant distribution of meteoroids encountering the Earth, *Adv. Space Res.*, submitted, (1996).

Unispace Kent (McDonnell, J.A.M. and Zarnecki, J.C.), Mare Crisium (Stevenson, T.J. and Deshpande, S.P.), Space Applications Services (Carey, W.C.), Maag, C.R., and ONERA/CERTS-DERTS (Mandeville, J-C), Prepared by Collier, I., Griffiths, A.D., Kay, L., Shrine, N. and Yano, H.: EuReCa Meteoroid and Debris Impact Survey, ESA/ESTEC Contract Report, **Contract No: 10522/93/NL/JG,** Noordwijk, the Netherlands, (1994).

Yano, H.: Cosmic Dust Collectors and Detectors (CDCD) for the Japan Experiment Module-Exposed Facility (JEM-EF), *Proc. 19th Int. Symp. on Space Tech. and Sci.*, 1017–1028, (1994).

Yano, H. and Kibe, S.: Post flight analysis program of retrieved spacecraft, *Proc. 19th Int. Symp. on Space Tech. and Sci.*, 893–904, (1994).

Yano, H.: The Physics and Chemistry of Hypervelocity Impact Signatures on Spacecraft: Meteoroids and Space Debris, **Ph.D. Thesis,** University of Kent at Canterbury, Kent, U.K., (1995).

Yano, H., Kibe, S., Neish, M.J. and Deshpande, S.P.: Meteoroid and space debris impact analyses on space flown components in Japan, *Proc. 20th Int. Symp. on Space Tech. and Sci.*, accepted, (1996).

Zook, H.A.: Meteoroids, space investigations, Astronomy and Astrophysics Encyclopaedia, (*edit.*) Maran, S., Van Nostrand, New York, 441–444, (1992).